Glass Europe Vol. 4 (2026) 1-28

https://doi.org/10.52825/glass-europe.v4i.2861

Submitted: 15 Jul. 2025 | Accepted: 22 Dec. 2025 | Published: 04 Feb. 2026

Defossilization of Industrial Glass Production via Carbon Capture and Utilization of Flue Gas

Techno-Economic and Ecological Evaluation of a Carbon Cycle Process Based on Synthetic Methane

Ferdinand Drünert[1,*], Yoga Rahmat[2], Bernhard Fleischmann[1], and Ralph-Uwe Dietrich[2]

[1]Hüttentechnische Vereinigung der Deutschen Glasindustrie (HVG) e.V., Germany

[2]German Aerospace Center (DLR), Institute of Engineering Thermodynamics, Stuttgart, Germany

*Correspondence: Ferdinand Drünert, info@hvg-dgg.de

Abstract. The glass industry faces significant challenges in achieving carbon neutrality due to its reliance on fossil fuels and process-related CO_2 emissions from raw material decomposition. While most defossilization efforts focus on CO_2-neutral heating, batch-related emissions remain largely unaddressed. This study investigates a closed carbon cycle approach for glass manufacturing by integrating carbon capture and utilization (CCU) with power-to-gas technologies. The proposed process captures both combustion- and batch-related CO_2 emissions and converts them into synthetic natural gas using renewable hydrogen. The techno-economic model, based on a typical oxy-fuel container glass furnace (300 t per day) and current (2022) German market conditions, covers all key process steps: flue gas cleaning, CO_2 separation, hydrogen production via electrolysis, and methanation. Results show that more than 99 % of scope 1 emissions and about 62% of scope 1+2 emissions can be abated. However, the process is associated with high energy demand and costs, with energy supply alone amounting to €559 (2022) per metric ton glass at an electricity price of €60 per MWh. The cost of CO_2 abatement is estimated at €1132 (2022) per metric ton. While all process steps are based on established industrial technologies, the overall economic viability remains highly sensitive to electricity prices and further technological improvements. The approach is especially relevant for high-quality glass production with low cullet content and in regions with abundant renewable electricity.

Keywords: CO_2-Neutral Glass, Carbon Capture and Storage/Utilization, Techno-Economic Assessment

List of Abbreviatons

AEL	alkaline electrolysis
AEM	All-electric melter
BECCS	bioenergy with carbon capture and storage
BP	byproduct
DACCS	Direct air carbon capture and storage
CAPEX	capital expenditures
CCS	Carbon Capture and Storage
CCU	Carbon Capture and Utilization
CCUS	Carbon Capture and Utilization / Storage
CEPCI	chemical engineering plant cost index
CW	cooling water
DH	district heating
EU ETS	European Union Emission Trading System
FCI	fixed capital investment
FLh	full load hours
GHG	greenhouse gases
GWP	global warming potential
HI	heat integration
LCOH	leveled cost of hydrogen
LHV	lower heating value
Nb-CDR	nature-based carbon dioxide reduction
NG	natural gas
NPC	net product cost
NRU	nitrogen removal unit
OPEX	operational expenditures
PEM	proton exchange membrane electrolysis
PH	preheating
SOEC	solid oxide electrolysis cell
P2G	power to gas
SC	steam cycle
SNG	synthetic natural gas
TEPET+	DLR's Techno-Economic and Ecological Process Evaluation Tool
TREMP™	Topsøe Recycle Energy-efficient Methanation Process

1. Introduction

Climate change represents one of the most pressing challenges of our time. Since society first recognized the implications of the greenhouse effect, we have witnessed a growing impact of greenhouse gases (GHGs) on the global climate, accompanied by an escalation of environmental hazards [1]. Recent studies indicate that previous and unavoidable future human-induced emissions will result in a permanent global average income reduction of 19 % over the next 26 years, compared to a scenario without anthropogenic climate change [2]. To mitigate further societal costs, the international community has committed to "…holding the increase in the global average temperature to well below 2 °C above pre-industrial levels…" [3]. This goal is approximately equivalent to a 20-year global average temperature of 16 °C [4]. The European Union Emissions Trading System (EU ETS) serves as a key instrument in this effort, setting a cap on GHG emissions within the EU through tradable allowances [5]. Market participants can purchase these allowances, creating an effective incentive to limit emissions [6]. As CO_2 accounts for about 78 % of the anthropogenic greenhouse effect [7], all GHG emissions are expressed as metric tons of CO_2 equivalents (t_{CO_2eq}). In contrast to the anthropogenic GHG emissions, only a few processes can effectively reduce GHG emissions, most notably among these direct air carbon capture and storage (DACCS), bioenergy with carbon capture and stor-

age (BECCS) and nature-based solutions for carbon dioxide removal (Nb-CDR) [8]. Each approach presents challenges including high water consumption, significant land-use, or substantial energy demand [9]. This results in considerable societal costs (land-use for Nb-CDR or BECCS) and economic burdens (BECCS, DACCS), alongside high energy consumption, particularly for DACCS. The combined potential of BECCS and DACCS to generate negative CO_2 emissions is limited, estimated between 0.3 to 1.9 Gt CO_2 annually by 2050 [10], [11]. Projections suggest that carbon capture and storage (CCS) technologies could cost between \$100 to \$825 per metric ton of CO_2 by 2050 [10], [12], [13].

Industrial processes, in particular, remain significant sources of GHG emissions. In 2023, the sectors industrial combustion and processes in the EU27 contributed approximately 508 Mt_{CO_2eq} [14]. Where process electrification is not feasible, hydrogen and its derivates represents promising alternatives to reduce GHG emissions [15]. However, many energy-intensive industries – such as steel, cement and glass – emit additional GHGs through process-related chemical reactions, necessitating carbon capture and utilization/storage (CCUS) technologies to achieve net-zero CO_2 emissions [16], [17], [18]. Within this context, the EU27 glass industry alone accounted for 21 Mt_{CO_2eq} in direct (Scope 1) emissions in 2021 [19], with about 25 % arising from batch decomposition. While recent initiatives have demonstrated the feasibility of CCS in the cement sector [20] and direct hydrogen reduction in steel production [21], the glass industry currently lacks a comprehensive approach for eliminating all CO_2 emissions. Most flagship projects concentrate on CO_2-neutral heating methods – such as hydrogen combustion [22], all-electric heating [23], or hybrid furnaces [24], combining hydrogen combustion and up to 80% electric boosting [25] – yet they defer addressing the challenge of unavoidable batch-related CO_2 emissions. To date, batch emissions are primarily mitigated by increasing cullet usage which decreases scope 3 CO_2 emissions by about 670 kg per metric ton cullet [26], and considering pre-calcined raw materials [27], [28], [29]; however, cullet availability limits these options, as losses during collection and processing reduce the amount of suitable recycled glass [30]. Analogously, pre-calcined raw materials mainly shift emissions upstream, rather than decrease overall emissions, although scope 3 emissions may benefit from carbon capture technologies with increased scaling, higher resource purity and decreased transportation emissions. Large-scale, low-cost, carbonate-free raw materials are not available yet, and the potential of CCUS for the glass sector remains underexplored in the literature, with the exception of few CCS-based projects [31], [32]. Without a solution for both heat- and batch-related CO_2 emissions, expensive EU ETS allowances will have to be obtained in the future, leading to largely unpredictable costs for the glass industry in 2045.

In this study, we investigate the potential of Carbon Capture and Utilization (CCU) for glass manufacturing by integrating carbon capture with power-to-gas (P2G) technologies. As a strictly continuous process with campaigns often lasting longer than a decade, glass production is a particularly suitable CO_2 supplier for the equally continuous fuel synthesis. This approach targets not only combustion-related but also batch-related CO_2 emissions, which are otherwise difficult to avoid. In rural regions without access to affordable hydrogen pipelines, glass plants can take advantage of abundant local renewable electricity, while local energy producers benefit from a stable industrial customer [33]. To enable a carbon-neutral glass production, we selected suitable, mature technologies for a production cycle with CCU based on methane and CO_2 as respective carbon carriers. Our design is especially advantageous for high-quality glass production with low cullet content, as it decouples the process from batch-related emissions. Although the glass melting process itself is strictly continuous and cannot be interrupted during a campaign, the concept does allow retrofitting the flue gas treatment of an existing furnace. To evaluate the feasibility of such a CO_2-neutral production route, we modeled the entire process chain, including flue gas cleaning, electrolysis and fuel synthesis, based on suitable and mature technologies. We then evaluated the techno-economic performance of this closed carbon cycle, ensuring that glass quality remains unaffected. In our approach, we abate CO_2 emissions by converting carbonates from batch raw materials (Na_2CO_3, $CaCO_3$ and $MgCO_3$) into a fuel surplus. Since these carbonates are not derived from renewable sources, we classify the resulting surplus as fossil-based. The following section outlines the

rationale for our technology selection and presents the main boundary conditions of our system.

2. Techno-economic approach to a carbon cycle process

2.1 Model description

Our model integrates five modules to establish a closed carbon cycle for glass manufacturing: (1) the glass furnace serves as the core process unit; (2) flue gas purification captures raw CO_2 emissions; (3) the electrolyzer unit produces renewable hydrogen; (4) syngas purification prepares synthesis-grade H_2/CO_2 mixtures; and (5) the methanation unit converts syngas into furnace fuel. We selected each technology to ensure seamless integration with both upstream and downstream units. For instance, we tailored the methanation unit (5) to match the glass furnace's fuel demand (1), while designing gas purification steps (2, 4) to meet stringent CO_2 specifications for methanation (5). Figure 1 illustrates the process chain schematically.

We developed the process chain in three stages: First, we used a Python-based simulation to model chemical interactions, define initial mass flows, and identify enrichment dynamics within the carbon cycle. Next, we constructed a detailed thermodynamic and kinetic model of all unit operations using Aspen Plus®. Finally, we embedded the Aspen model into DLR's in-house Techno-Economic and Ecological Process Evaluation Tool (TEPET+) to calculate net product costs, fixed capital investment and abatement costs. The decomposition of glass batch materials introduces CO_2 into the process chain, generating a methane surplus as byproduct (BP). Table 1 summarizes key parameters for the techno-economic evaluation, including plant location, CEPCI and exergy demand. For further information on the selected equipment functions, see Rahmat et al., 2025 [34].

For the estimation of SNG net production cost (NPC_{SNG}), we adopted a projected long-term electricity price of €60 per MWh_{el} (2022) for Germany [35]. As electricity dominates the cost structure, we conducted a sensitivity analysis to evaluate NPC_{SNG} variations against electricity price fluctuations (section 5.4). Additionally, we calculated CO_2-abatement costs using Equation 1, where scope 1 CO_2(x) (that is direct emissions at the plant) differentiate synthetic fuel from natural gas. These abatement costs imply that the synthetic fuel surplus is processed with implemented carbon capture and storage technologies.

$$CO_2\ abatement\ cost\ \left[€_{2022}\ t_{CO_2}^{-1}\right] = \frac{NPC_{synfuel} - NG\ price}{CO_{2_{NG}} - CO_{2_{synfuel}}} \quad (1)$$

Germany's projected 2030 renewable electricity mix (37.6 % onshore wind, 23.9 % offshore wind, 32.5 % photovoltaics, 2.4 % hydropower, 3.6 % bioenergy) [36] meets the system's demand. We derived the global warming potential (GWP) of this mix from literature-based CO_2 footprints for each energy source [37]. Additionally, we considered water disposal costs of €1.31 per cubic meter, as stated in the literature [38].

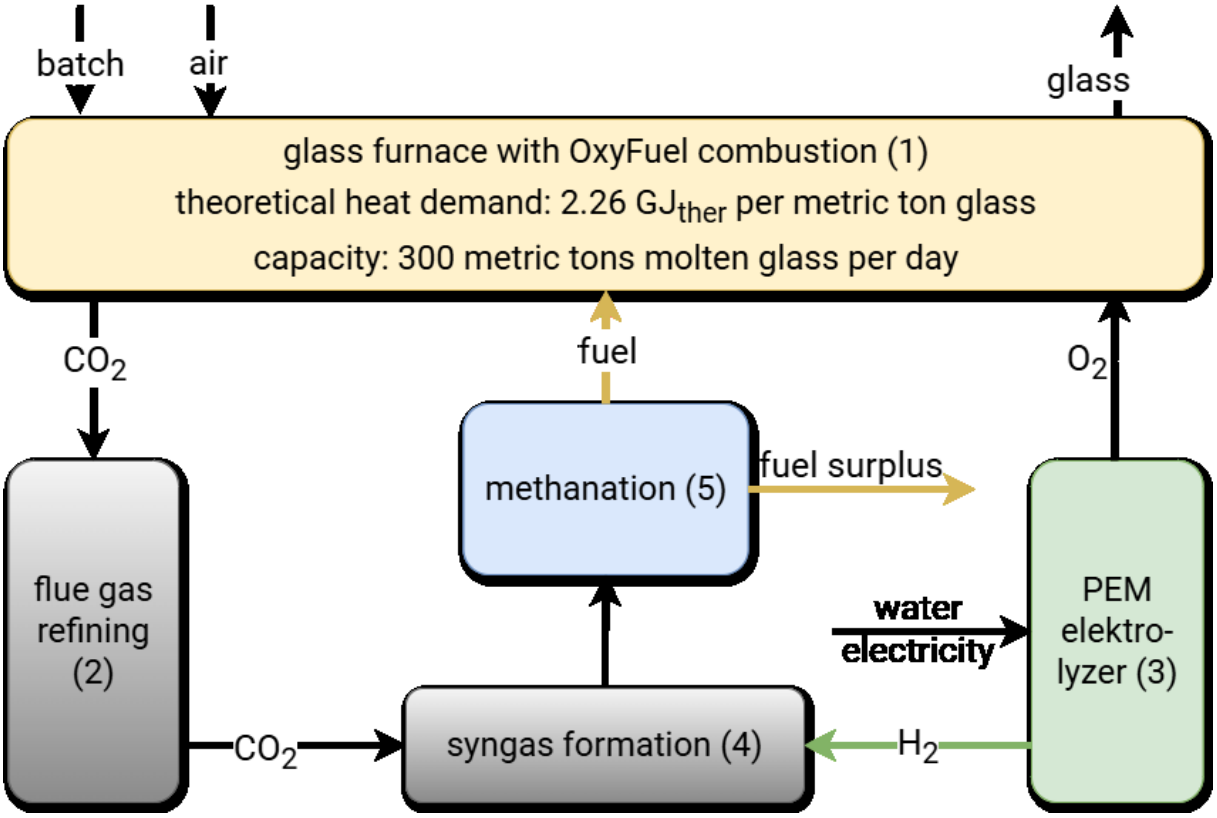

Figure 1. *Schematic overview of the model design.*

We prioritized maximizing synergy effects through heat integration – for instance, utilizing methanation waste heat for feedstock preheating. Details about the Aspen Plus® equipment and thermodynamic models employed are given in [34].

Table 1. *Key parameters for techno-economic assessment.*

Parameter	
Plant location	Germany
Secondary product (surplus)	Methane
Reference year	2022
CEPCI (2022)	816
Currency	€
Full load hours (FLh)	8760 h a^{-1}
Plant lifetime	15 a
Interest rate	7 %
Labor cost	€45.1 h^{-1}
Nominal labor index (2022)	113
Assumed natural gas price (HHV / LHV; for reference)	€125.72 / €138.29 MWh^{-1} [39]

2.2.1 Glass furnace

We constructed our model based on a typical container glass production line producing 300 t molten glass daily. Given the major influence of energy efficiency and flue gas volume on net production costs, we employed oxy-fuel combustion to enhance process efficiency. We accounted for a 1% fuel increase per year due to furnace degradation. Unless otherwise noted, all values refer to the average-aged furnace.

The specific glass type minimally affects the overall process chain. For this study, we selected amber glass because it poses particular challenges for all-electric melting [40]. According to the best available technologies report [41], oxy-fuel furnaces achieve specific heat consumption (LHV) of 3.0 to 3.5 GJ_{SNG} per metric ton of molten glass. This includes wall losses, oxidizer / SNG preheating, and 70% cullet content. The reported range incorporates up to 15% electrical boosting, which was not considered in our model. Since these data derive from only two plants, we adopted a more conservative specific heat consumption (LHV) of 4.18 GJ per metric ton of glass at a lower cullet content of 50 % in a new furnace (see Table 2). This figure breaks down into a theoretical energy demand of 2.26 GJ [42], [43], 0.87 GJ lost through wall heat losses, 1.29 GJ lost via flue gas, and 0.25 GJ energy saved by preheating oxygen and fuel. For a degraded, end-of-life furnace, fuel needs rise to approximately 4.8 GJ SNG (LHV) per metric ton of molten glass, comprising 1.45 GJ wall losses, 1.9 GJ flue gas heat loss, and 0.3 GJ energy saved by fuel and oxygen preheating. To capture cost implications, we set the oxidation rate λ to 1.02, corresponding to 1 % oxygen content in the hot flue gas. Additionally, we assumed a 1 % leak air rate, reflecting typical air ingress contributing to flue gas composition. Under these conditions, the total combustion power (LHV basis, average-aged furnace) reaches 15.6 MW_{th} for a daily throughput of 300 t molten glass, resulting in annual CO_2 emissions of approximately 35 kt.

Table 2. *Parameter set for the furnace model*

Parameter	
Furnace capacity	300 t molten glass per day
Combustion type	Oxy-Fuel combustion
Residual oxygen in flue gas (λ value)	1 % (λ = 1.02)
Leak air rate	1.5 % of the flue gas
Glass type	Amber container glass
Cullet rate	50 %
Efficiency loss per year	1%
Fuel requirement (HHV) of the furnace (n. / av. / 15y)	4.64 / 4.98 / 5.39 GJ t^{-1}_{glass}
Fuel requirement (LHV) of the furnace (n. / av. / 15y)	4.18 / 4.48 / 4.85 GJ t^{-1}_{glass}
Electric boosting	Not considered
Fuel / oxidizer heat-up	5.1 % of total heat input
Wall losses (new / average / after 15 years)	0.88 / 1.15 / 1.44 GJ t^{-1}_{glass}
Efficiency (heat-to-melt, n. / av. / 15y)	46 % / 43 % / 40 %
Flue gas heat loss (n. / av. / 15y)	1.74 / 1.86 / 1.98 GJ t^{-1}_{glass}
Quenching th. power (water quenching, 1450°C to 1000°C)	1.6 / 1.7 / 1.8 MW_{th}
Assumed heat exchanger power (1000°C to 200°C)	3.0 / 3.2 / 3.4 MW_{th}

The flue gas results from both the decomposition of the glass batch (“batch related CO_2 emissions”) and the combustion of SNG (“heat related CO_2 emissions”). The initial flue gas composition, defined by combustion products and batch decomposition products, is shown in Table 3. To sustain the desired glass melt, the process in the average-aged furnace generates a total flue gas volume of approximately 6290 Nm^3_{flue} per hour at 1450 °C, corresponding to a

heat flow rate of 6.4 MW_{th}. This flue gas composition defines the boundary conditions for the subsequent purification steps.

Table 3. *Flue gas composition and contaminants as modeled after leaving the furnace area (1), raw CO_2 after wet scrubber and NRU (2) and syngas formation (3, with additional 80% H_2). Additionally, typical pipeline limits for CO_2 transportation (corrosion prevention) are displayed in the last column.*

	Flue gas (1)	Clean CO_2 (2)	Syngas (4)	Pipeline guidelines
CO_2	37 %vol	90 %vol	20 %vol	>= 95 %vol
H_2O	61 %vol	7 %vol	0.07 %vol	< 630 ppm(vol)
N_2	1.3 %vol	0.07 %vol	0.03 %vol	<= 4%vol
O_2	1.0 %vol	2.4 %vol	< 0.01 %vol	<= 10 ppm(vol)
SO_2	2300 mg Nm^{-3}	5 mg Nm^{-3}	< 0.1 mg Nm^{-3}	<= 35 ppm(vol)
NO_x	660 mg Nm^{-3}	130 mg Nm^{-3}	< 10 mg Nm^{-3}	<= 10 ppm(vol)
HCl	150 mg Nm^{-3}	0.4 mg Nm^{-3}	< 0.01 mg Nm^{-3}	<= 10 ppm(vol)
CO	150 mg Nm^{-3}	30 mg Nm^{-3}	30 mg Nm^{-3}	<= 10 ppm(vol)
HF	130 mg Nm^{-3}	0.02 mg Nm^{-3}	< 0.01 mg Nm^{-3}	<= 10 ppm(vol)
dust	550 mg Nm^{-3}	< 0.1 mg Nm^{-3}	< 0.1 mg Nm^{-3}	<= 10 ppm(vol)

After heat exchange, the furnace module delivers flue gas at 200 °C, enabling efficient integration with the gas cleaning stage. As the flue gas exits the furnace at 1450 °C, a heat recovery step cools it to 200 °C, with entry temperatures of 1000 °C after quenching. This temperature range is suitable for steam cycle (SC) electricity generation. Further cooling is avoided to prevent sulfuric acid condensation from SO_2 in humid gas. The interval from 1450 °C to 1000 °C is not utilized for heat recovery; instead, temperature quenching is achieved by water injection into the flue gas stream.

2.2.2 CO_2 recovery from flue gas

Fuel synthesis requires high-purity feedstocks. Effective flue gas purification, reducing pollutant concentrations to the ppb range, is essential to protect the Ni-based catalysts used in SNG synthesis. This is particularly true for sulfur, halides and dust, all of which pose high risks of catalyst deactivation. Nitrogen and oxygen, although less problematic, reduce synthesis efficiency but do not deactivate the catalyst. CO_2 separation from oxy-fuel flue gas follows two main approaches:

One approach focuses on direct CO_2 removal using technologies such as swing adsorption or amine scrubbing processes [44]. Due to non-ideal adsorption rates, this inevitably results in some CO_2 loss to the atmosphere [45], [46], [47]. In this model, we did not consider CO_2 isolation because the comparably high SO_2 levels, originating from fining agents used in glass production, would degrade amine carriers and increase operational costs [48]. Instead, we prioritized the removal of residual flue gas components.

Problematic components can be removed by cooling the flue gas, as vapor condensation further concentrates CO_2. While increasing amounts of flue gas components raises technology costs, treating individual fractions allows the process chain to be optimized for the requirements of fuel synthesis [49]. We therefore deliberately separated the CO_2 recovery from flue gas (flue gas refining, see Figure 1) and the syngas preparation to enable a targeted optimization of each purification step according to the specific requirements of the downstream fuel synthesis.

CO_2 recovery is implemented in two steps. First, a lime based wet scrubber achieves significant removal of sulfur, halides, and dust from water-rich flue gases. Operating at 20 to 80 °C and pH 5 to 7, it simultaneously cools the gas [50]. Typical removal rates for undesired contaminants reach 95 to 99 % [51]. Dust is mechanically separated on the droplet surface of the lime slurry, while SO_2 and halides react chemically with Ca^{2+} ions to form the respective salts.

The lime slurry, at average temperatures of 15 °C, cools the hot flue gas to 40 °C, as required for the downstream membrane filter. The spent slurry is filtered for water recovery. The selected parameters for the wet scrubber are summarized in Table 4.

Table 4. *Selected parameters of the wet scrubber calculation.*

Parameter		Sources & Comments
Wet scrubber type	Spray tower (CaCO3)	[51], [52]
Inlet temperature flue gas	200 °C	From furnace heat recovery
Outlet temperature flue gas	40 °C	Operating temperature NRU
Inlet temperature lime slurry	15 °C	
Outlet temperature slurry waste	40 °C	
pH value	6 – 7	[52]
Required cooling power (n/av/15y)	2.9 / 3.2 / 3.4 MW_{th}	from 200°C to 40°C
Required cooling water	34 t_{water} MW^{-1}cooling	from 200 °C to 40 °C
Required $CaCO_3$ slurry	1.05 $mol_{CaCO_3}/mol_{Hal+SOx}$	
Removal rate in simulation	99 %	dust, SO_x, halides; [52]
Minimum pollutant rate (outlet)	10 ppm_{vol} (HF: 1 ppm_{vol})	[51]
Pressure drop	1.5 kPa	[52]
CO_2 total pollutant load	Σ pollutants: 120 ppm_{vol}	Dry gas

In the second step, the CO_2-rich gas stream passes through a membrane filter for nitrogen removal. Continuous air leakage into the furnace leads to progressive nitrogen enrichment in the process cycle, which can significantly reduce synthesis efficiency and thus necessitates dedicated nitrogen removal. Nitrogen removal units (NRU, Table 5) are standard equipment for natural gas upgrading and enable removal of up to 93 % of N_2, with 99.9 % of the CO_2 remaining in the retentate [53], [54].

Table 5. *Parameters of the nitrogen removal unit.*

Parameter		Sources & Comments
Nitrogen removal equipment	Membrane filter	[55]
Temperature level	40 °C	
Removal rate N_2 (permeate)	92.75 $\%_{vol}$	[56], [57]
Loss rate CO_2 (in permeate)	0.01 $\%_{vol}$	[56], [57]

The CO_2 product quality after recovery meets transportation standards for carbon capture and storage [58], [59], provided a final drying step is included.

2.2.3 Hydrogen synthesis

Hydrogen acts as the key reducing agent in fuel synthesis and can also serve as a fuel for the glass furnace [22]. As the most mature technology to produce hydrogen, water electrolysis is primarily constrained by the availability of green electricity rather than feedstock supply. The most promising electrolysis technologies are high-temperature electrolysis (solid oxide electrolysis cell, SOEC), alkaline electrolysis (AEL) and proton exchange membrane electrolysis (PEM). While SOEC technology currently suffers from limited stack lifetimes and high production costs, AEL and PEM electrolyzers are already commercially available at industrial scales (AEL: GW, PEM: MW). All three technologies are expected to experience significant cost reductions in the coming decades, primarily due to improvements in stack lifetime and efficiency, with the most pronounced decrease projected for SOEC [60].

Recent studies indicate that the flexibilization of hydrogen production can significantly impact overall process economics [61], [62]. This operational flexibility, typically reflected in the leveled cost of hydrogen (LCOH), underscores the increasing importance of operating expenditure (OPEX) relative to the fixed capital investment (FCI) – particularly under fluctuating renewable electricity prices. Given the inherently volatile nature of renewable electricity supply, flexible hydrogen electrolysis is a potential strategy to adapt production to variable power availability. In this context, we investigated whether such operational flexibility offers economic or technical benefits. The PEM technology is especially well-suited for dynamic operation [63], making it ideal for simulating non-continuous hydrogen production under fluctuating renewable electricity supply, while maintaining a stable fuel synthesis output. However, according to 2022 data, PEM electrolyzers are associated with higher capital costs (€1.515M per MW produced hydrogen) and a slightly lower efficiency (51 % based on LHV) [64] than AEL systems (€1.000M per MW produced hydrogen, 53.3 % LHV) [65], [66]).

2.2.4 High-purity syngas

Unlike in transportation applications, the CO_2 purity achieved in the previous recovery step does not meet the stringent requirements for catalytic methanation. Nickel-based catalysts, typically supported on alumina (Al_2O_3), are highly sensitive to impurities and prone to corrosion [67], [68], [69]. To prevent catalyst poisoning, only trace amounts of halides, dust, or sulfur – generally below 10 ppb_{vol} – are tolerated in the reactor feed [70]. Although oxygen is less critical, lower concentrations are preferred to minimize efficiency losses.

Both CO_2 and H_2 are required for the methanation process. We therefore combine these gases via catalytic hydrogenation at 260 °C to produce syngas suitable for downstream conversion [71]. In this process, SO_2 and O_2 react with hydrogen to form H_2S and H_2O, respectively. Unlike SO_2, removing H_2S from feed gases is a well-established industrial practice, for example in Fischer-Tropsch synthesis, typically performed using ZnO guard beds [72]. Similarly, activated alumina guard beds are commonly used to remove halides [72].

2.2.5 Methanation

The glass furnace requires a continuous and reliable fuel supply over multiple years. To reflect this, our simulation focuses on a steady state methanation process for optimal energy management. In this simulation, the methanation reaction was simplified to Equation 2. Here, four molecules of hydrogen are needed to convert one molecule of CO_2 into methane, releasing about 165 kJ per mol. To avoid catalyst poisoning, the feed gas must contain less than about 100 ppb_{vol} of halides, sulfur and dust and less than 10 ppm_{vol} oxygen [73].

$$\mathrm{CO_2} + 4\mathrm{H_2} \rightarrow \mathrm{CH_4} + 2\mathrm{H_2O} \qquad \Delta H^0 = -165{,}0\, kJ/mol \tag{2}$$

Efficient cooling is required to ensure high methane yields due to the exothermic nature of the reaction. The Topsøe Recycle Energy-efficient Methanation Process (TREMP™) is particularly suited for this purpose, employing a cascade of three to four fixed-bed reactors to maximize energy recovery and process efficiency [74].

The product composition depends on the reaction parameters. In our simulation, we targeted a product gas containing 94.5 % methane, 3.5 % hydrogen, 1.3 % carbon dioxide, and trace amounts of carbon monoxide, nitrogen, and water. This quality is achieved in four nickel-catalyzed reactor stages at 700 °C, 530 °C, 400 °C and 420 °C, with cooling after each stage. The final product leaves the process at 250 °C and 3 MPa.

2.2 Final process cycle

The final process cycle encompasses all selected technologies and interconnects the respective educt and product streams. Figure 2 illustrates the process flow diagram for the complete

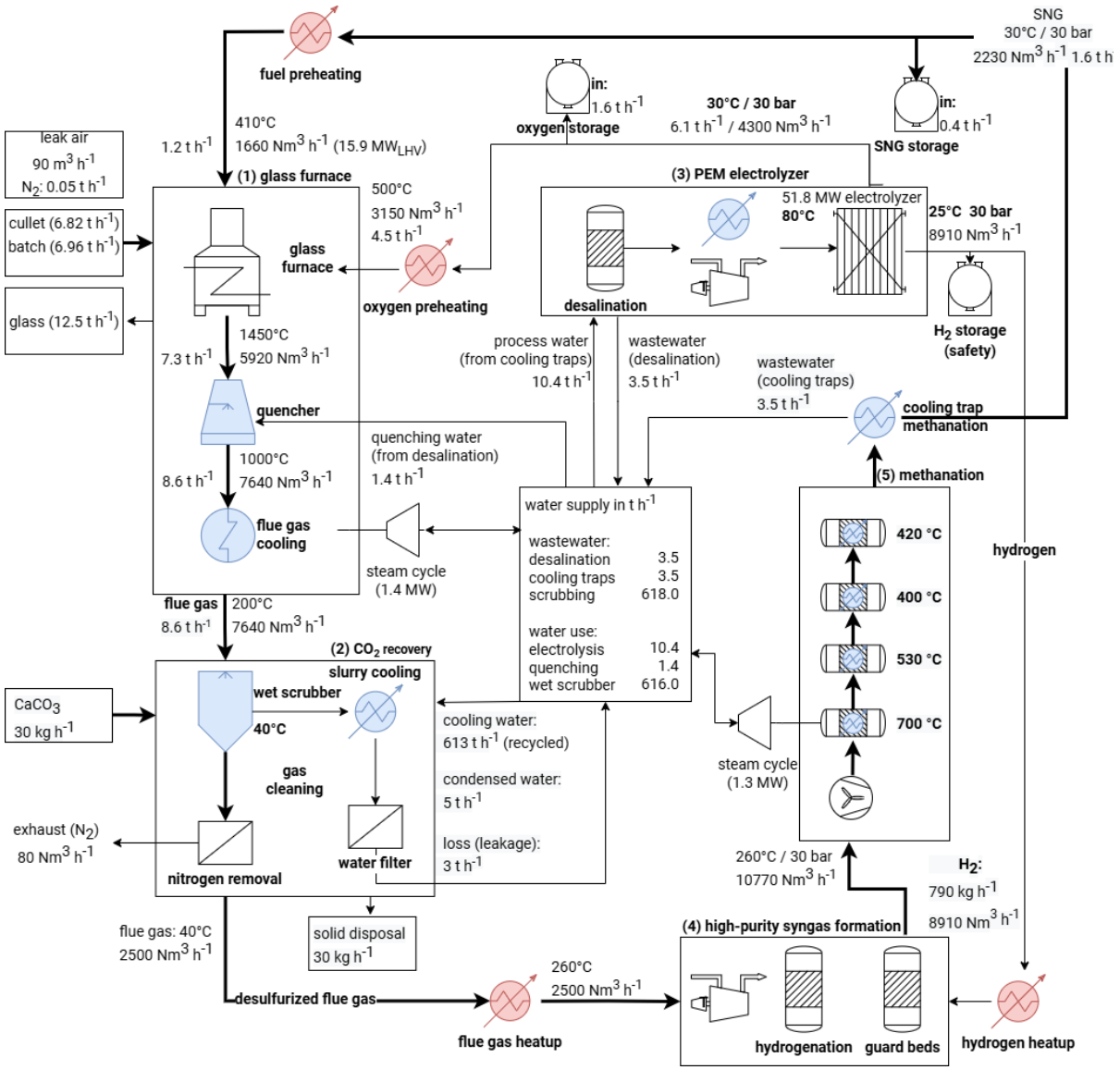

Figure 2. *Process flow diagram of the complete cycle with an average-aged furnace. Bold lines symbolize the path of the carbon cycle. Heat exchangers with a cooling function are displayed in blue, while heating is shown in red. All values are given in the model's scale.*

cycle, detailing all relevant quantities and product volumes. Centrally positioned, a water management unit oversees both wastewater treatment and the distribution of service water throughout the processes. It supplies service water to the wet scrubber in (2), collects wastewater from various process streams, and recovers condensate from the cold trap in the methanation unit (4). In addition, the unit provides water to the electrolyzer and manages quenching operations for feedstock streams as required.

2.3 Cost optimization at flexible hydrogen production

Fuel synthesis demands a constant hydrogen supply of 790 kg per hour (63 kg_{H_2} per metric ton molten glass). To introduce flexibility into hydrogen production, we implement both hydrogen storage and an increased production capacity. Although larger storage volumes result in efficiency losses due to compression and boil-off, they enable us to take advantage of lower electricity prices. Because electricity prices are typically set one day in advance on the day-ahead market, we optimize the electricity consumption using the Bellman equation on historic day-ahead market data [75], [76]. In Equation 3, the value function *V* for optimal electricity use

depends on the electricity price at a given hour (*t*) and the current storage level (*s*). We determine *V* recursively using the cost function of the subsequent storage level and electricity price *V(t+1, s'):*

$$V(t) = \min_{a}[C(t,s,a) + V(t+1,s')]\,, \tag{3}$$

where *C(t, s, a) represents* the immediate cost of action *a*. This approach allows us to evaluate electricity prices from the day-ahead market in a recursive framework. We account for energy consumed during hydrogen compression, assuming 10 % of the produced hydrogen's LHV as an additional energy cost [77]. We also include a boil-off rate of approximately 0.08 % of the current storage level, equivalent to 2 % over a 24-hour period [78]). Applying this cost function, we analyzed electricity prices from 2019 to 2024 to identify potential OPEX reductions. To reduce the impact of seasonal and weather-related fluctuations, we set a target end storage value based on the day's median ($median_{now}$) electricity price compared to the preceding 14 daily *median* values (see Equation 4).

$$storage_{target} = max(storage)\ \frac{median_{now} - min(median)}{max(median) - min(median)} \tag{4}$$

3. Technical analysis

3.1 Technological readiness level of the total process

Technical maturity was a mandatory requirement for the investigated process cycle. Consequently, all selected technologies are either established industrial standards or have been proven in similar applications. We integrated a PEM electrolyzer, water quenching, wet scrubbing, a nitrogen removal unit, guard beds, hydrogenation, and methanation into the glass production cycle. Furthermore, we connected all hot and cold process streams through heat integration and employed a steam cycle for waste heat recovery.

In contrast, conventional glass production does not require such extensive gas cleaning. In Germany, exhaust gases from industrial glass production must comply with the TA Luft, as specified in the 44. BImSchV (German Federal Immission Control Ordinance). While the regulation sets strict limits for nitric oxides in flue gas, the requirements for syngas purity in SNG production are even more stringent, permitting only a few mg per cubic meter of SO_2, halides, or dust. Wet scrubbers, which do not reduce NO_x levels but are effective for removing dust and sulfur, are therefore uncommon in the glass industry. Likewise, the synthesis of methane from glass production flue gas has not yet been implemented, and none of the proposed process steps have been tested in this context. As a result, the process chain outlined here requires further investigation before it can be considered industry ready, for example in a pilot plant. At present, the process chain corresponds to technology readiness level 3.

3.2 Energy assessment and heat integration

Electric energy is the only external energy source for the entire process cycle. Most process steps require only small amounts of electric energy, with compressors consuming 300 kW_{el}, ventilation 60 kW_{el}, and both blowers and pumps about 3 kW_{el} each. Hydrogen compression for storage typically requires about 10 % of the hydrogen's LHV. However, we did not allocate these energy costs to the process cycle, since hydrogen storage is used only for maintenance and backup.

An overview of heat flows and heat integration (HI) is given in the grand composite curve (Figure 3) and the Sankey diagram (Figure 4). As heat integration is a key component to enable synergy effects in the process chain, we implemented a steam cycle (SC, assumed efficiency of 43 % at 200 bar, 41-550 °C) into the flue gas processing (SC2, 3.2 MW_{th}) and the first step of the fuel synthesis (SC1, 2.9 MW_{th}) to recover 2.7 MW_{el}. About 1.3 MW_{th} of the remaining

fuel synthesis steps can be used for internal heating, such as preheating (PH) of fuel, oxygen, and methanation reactor feed.

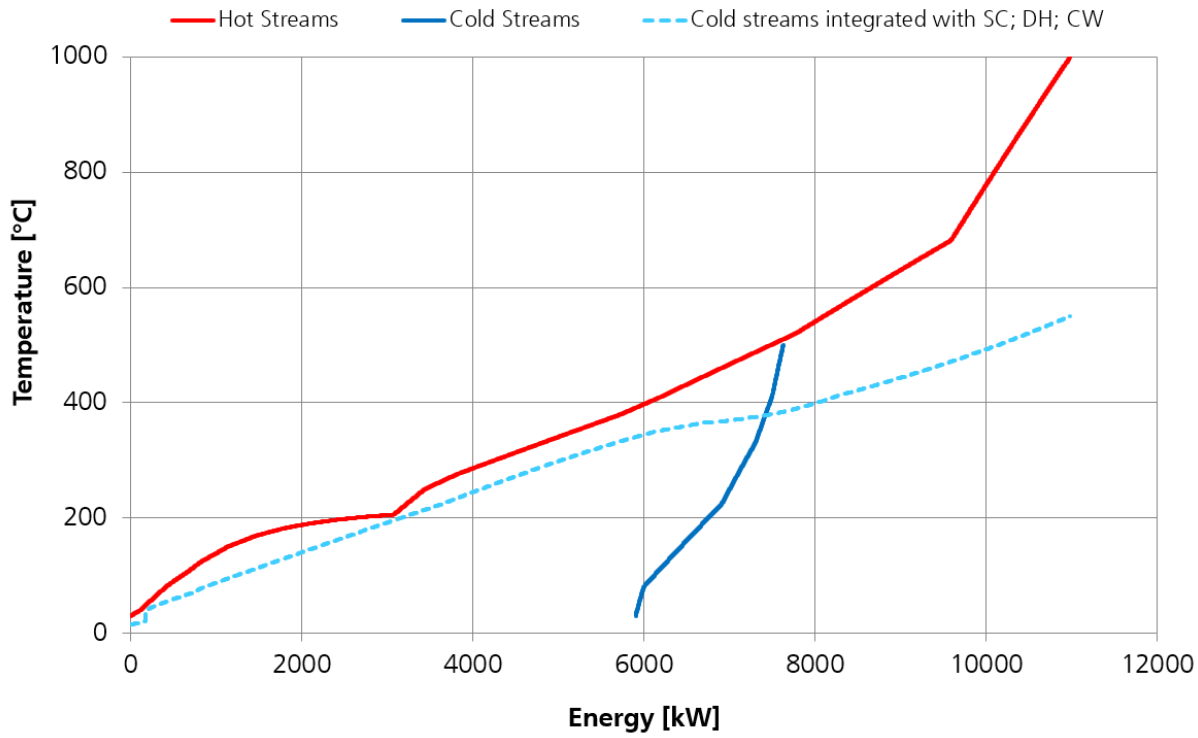

Figure 3. *Grand composite curves of the process cycle, with hot streams (red), cold streams (blue) and heat integrated cold streams (dashed).*

Overall, the fuel synthesis step provides 7.6 MW_{th} of hot streams and 0.4 MW_{th} of cold streams. The remaining process steps contribute another 3.8 MW_{th} integrable hot streams and 1.3 MW_{th} of cold streams. In total, the process cycle contains 11.0 MW_{th} of hot streams and 1.7 MW_{th} of cold streams, as shown by the grand composite curves in Figure 3. Heat integration (HI) is performed using a pinch analysis with a pinch temperature of 10 K. Since the available hot enthalpy streams exceed the cold streams, not all heat can be recovered internally. Therefore, we considered three integration options: a steam cycle, district heating (DH, 6 bar, 50-70 °C), and cooling water (CW, 1 bar, 15-20 °C) [79], [80].

Of 51.8 MW_{el} that are required to generate hydrogen for the process chain (see Figure 4), 18.5 MW_{SNG} and 0.9 MW_{th} (PH fuel and PH oxygen) are actively used for the melting process. 2.7 MW_{el} can be regenerated via steam cycle (SC 1 and SC 2), 0.8 MW_{th} (PH reactor feed and PH R4) is recovered in the fuel synthesis and 2.6 MW_{th} is available for district heating (DH), but this does not improve the overall energy balance. The remaining 30.1 MW_{th} cannot be recovered within the process chain.

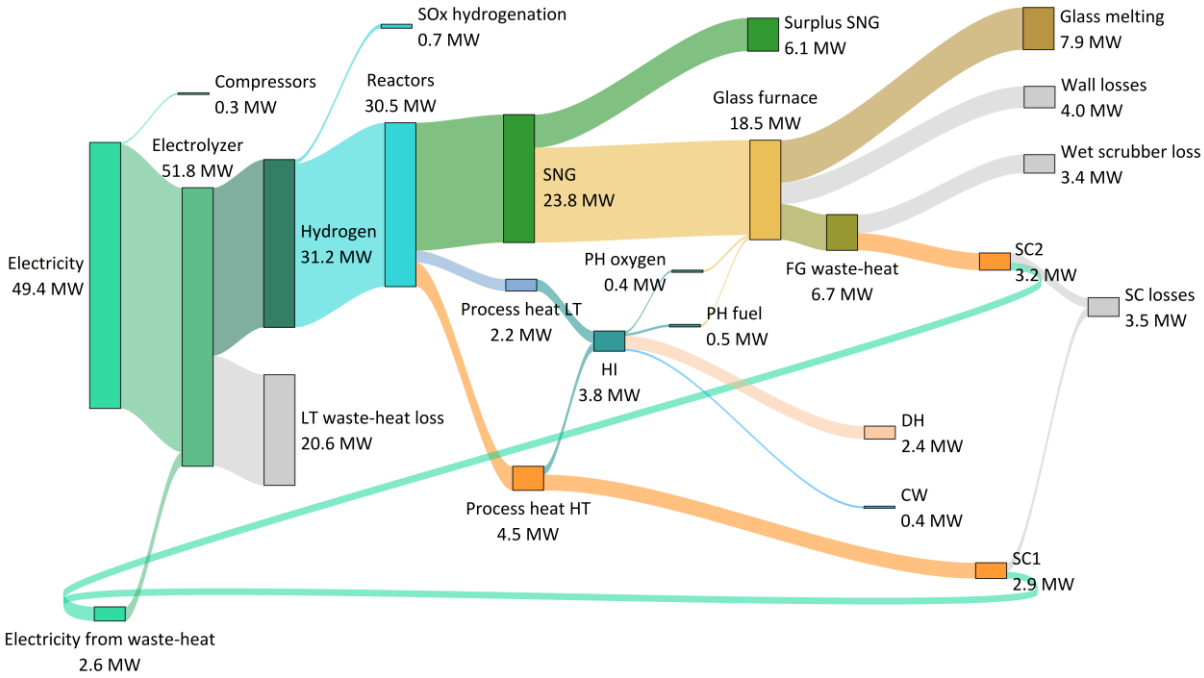

***Figure 4**. Energy flow diagram of the model's process chain based on the average-aged furnace.*

4. Ecological impact of the process cycle

The proposed process cycle relies exclusively on electricity as its external energy source. However, several resources are required to sustain continuous operation. We assess the ecological impact in three categories: water management, resource management, and CO_2 emissions.

4.1 Water management

Cooling water serves as the primary cooling agent throughout the process chain. Cooling demand arises in the methanation step, the steam cycles, the electrolyzer unit, and the flue gas treatment system (including wet scrubber, heat exchanger, and quencher). Additional water is necessary for the deionization of the electrolyzer feed. Wastewater arises not only from the cooling and condensation operations within the equipment but also from the deionization treatment of the electrolyzer feed water. Since other cooling-intensive processes are modeled with a closed cooling cycle, the required make-up water remains below 0.02 metric tons water per metric ton molten glass and is therefore negligible in this context. Table 6 summarizes the water balance for the main process steps.

Table 6. *Water balance of selected process steps.*

Process step	Water Demand [$t_{water}\ t_{glass}^{-1}$]	Wastewater [$t_{water}\ t_{glass}^{-1}$]	Comments
Electrolyzer	- 0.83	0.28	includes desalination
Flue gas quenching	- 0.11		
Wet scrubber	- 0.24	0.40	
Methanation		0.28	
Sum	- 1.18	0.96	

The proposed service water consumption significantly exceeds that of a standard glass manufacturing plant, making water use optimization a crucial consideration. Since the electrolysis module already incorporates several water purification steps, including water softening, reverse osmosis, membrane degassing, and electro-deionization [81], we expect that wastewater from wet scrubbing and methanation can be partially reused within the electrolyzer unit. Likewise, the increased mineral content resulting from the desalination process does not significantly impact flue gas quenching or wet scrubbers, preserving the potential to reduce water consumption and wastewater disposal costs. In this optimal scenario, the total water consumption could be reduced to approximately 0.2 t per metric ton of molten glass. However, to reduce complexity, we did not consider these options in the current study; instead, we estimated all costs for service water and wastewater disposal according to [38].

4.2 Resource management

The process chain requires only a few additional resources beyond electricity. However, chemical treatment is essential for the CO_2 purification, particularly for the removal of halides and sulfur. In our model, the wet scrubber provides primary purification: lime ($CaCO_3$) reacts with HCl, HF, and SO_x in the gas phase, forming $CaCl_2$, CaF_2 and $CaSO_4$, respectively. This step requires approximately 2.4 kg $CaCO_3$ per metric ton molten glass (260 t $CaCO_3$ per year), generating a similar amount of waste. Although we did not consider valorization of this waste, further use as, such as gypsum production, is possible.

Secondary purification relies on ZnO (14.4 g ZnO per metric ton molten glass, 1.5 t ZnO per year) and activated alumina (3.2 g Al_2O_3 per metric ton molten glass, 0.35 t Al_2O_3 per year) to remove residual sulfur and halides. Like in the primary step, we did not include valorization of the resulting waste (ZnO guard bed: 16.8 g per metric ton molten glass / 1.8 t per year, activated alumina guard bed: 4.8 g per metric ton molten glass / 0.53 t per year). Both materials can be regenerated by heat treatment, but due to the small quantities, this option was not considered.

The use of rare materials is another relevant aspect. While reactor materials, piping and others do not contain significant amounts of critical elements, catalysts for PEM electrolysis and methanation are more critical. PEM electrolyzers require platinum (40 to 150 g per MW and year / 1.9 to 7.2 kg total per year in this model) and iridium (50 to 700 g per MW and year / 2.4 to 33.8 kg total per year in this model) [82]. Methanation catalysts require about 650 t nickel per year [83].

4.3 Global warming potential (GWP)

We assess CO_2 emissions according to three categories (scopes): direct emissions controlled by the operator (scope 1), indirect emissions from electricity generation (scope 2), and other indirect emissions from upstream and downstream activities (scope 3) [84]. Only scope 1 emissions have to be compensated with EU ETS allowances and thus affect the glass production costs. Our analysis includes all scope 1 and 2 emissions directly related to the process chain.

Scope 1 emissions arise at the NRU, where membrane filters release 30 g CO_2 per metric ton molten glass (scope 1.4: fugitive emissions). There are neither stationary combustion (scope 1.1) nor process emissions (scope 1.3) in the process chain, and mobile combustion emissions (scope 1.2) were not included but must be considered in a real plant. The process chain does not require heat, vapor, or cooling energy inputs, but electricity input is significant at approximately 3.9 MWh per metric ton molten glass. Even when using "green" electricity, renewable sources are not entirely CO_2-neutral. The carbon footprint depends on the energy mix and ranges from 2 to 100 kg CO_2 per MWh. Here, we use an average value of 31.4 kg CO_2 per MWh, based on the assumed energy mix and the respective published emission factors [36], [37]. Thus, total scope 1+2 emissions for the modeled process chain amount to approximately 130 kg CO_2 per metric ton molten glass, compared to 339 kg CO_2 per metric ton molten glass, including 114 kg CO_2 from batch emissions, in a similar process without CCU.

5. Economic assessment

5.1 Capital expenditures (CAPEX)

The CAPEX analysis (Figure *5*) includes the estimation of equipment cost (EC) and fixed capital investment (FCI), following the procedure outlined by Rahmat *et al.* (2025) [34]. EC are determined using cost functions from the literature. Standard equipment, such as compressors, pumps, heat exchangers, flash drums, and storage tanks, is costed according to [38]. Cost functions for the fixed-bed methanation reactor, wet scrubber (WS), membrane systems, and hydrogen storage are sourced from [50], [56], [85], and [86], respectively. The FCI is calculated by multiplying the estimated EC by CAPEX cost factors, which account for installation, piping, instrumentation, electrical systems, and related expenses. Since the furnace itself remains unchanged, the furnace module was excluded from the FCI calculation. As the furnace degrades over time, the model includes all equipment required for the end-of-life furnace.

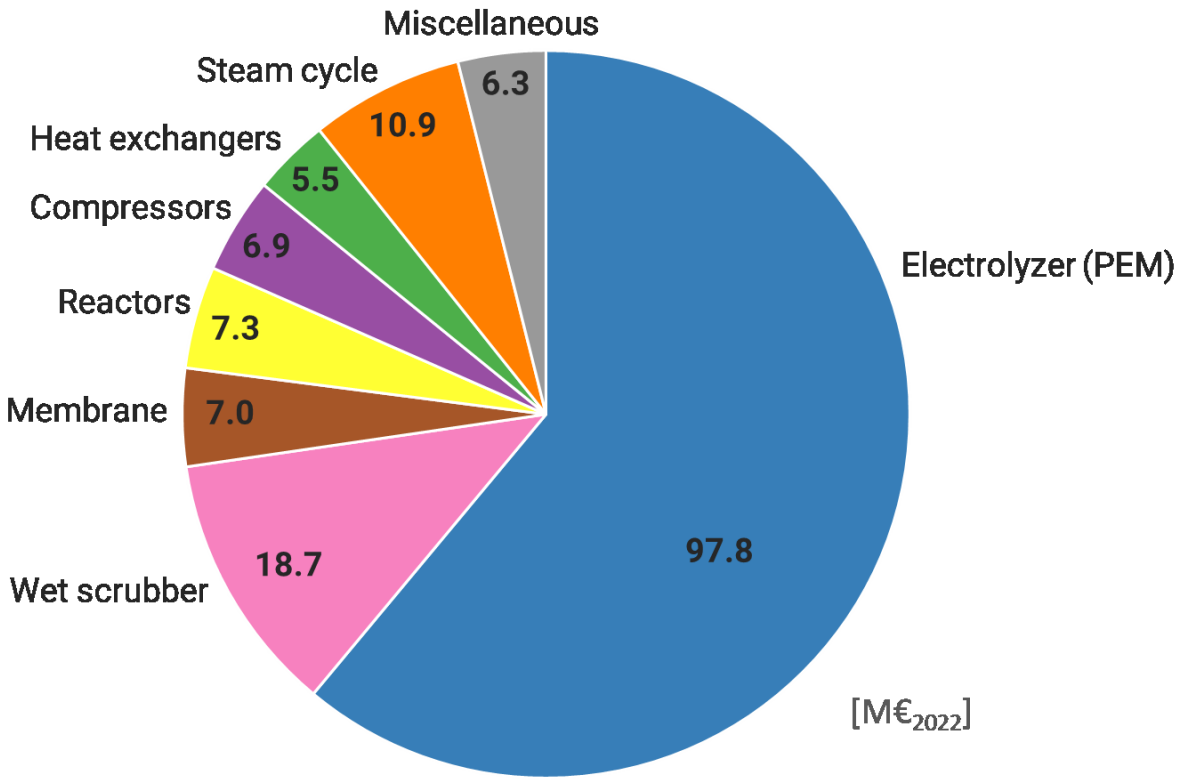

Figure 5. *CCU fixed capital investment in M€$_{2022}$*

The total FCI for the CCU plant amounts to €160.4M (2022), with 61 % of this investment allocated to the PEM electrolyzer. This substantial share is consistent with typical CCU or Power-to-X process that rely on electrolytic hydrogen. The wet scrubber accounts for approximately 11 % portion of the total FCI, a figure comparable to the investment required for the entire methanation process (2 % FCI share), which includes reactors, compressors, and heat exchangers. The steam cycle, which is integrated to recover heat from the TREMP™ process and supply electricity for internal consumption, represents 7 % of the total FCI. The annuity of the steam cycle is €1.28M per year (2022), indicating that its integration becomes economically viable at an electricity price of €54 per MWh_{el} (2022).

5.2 Net production cost (NPC)

In this study, we analyze the NPC of the CCU component within a theoretical glass plant. Since the investigated processes are additional to regular glass production, the resulting NPC replaces the NPC calculated with contemporary flue gas treatment and CO_2 allowance costs. Therefore, NPC is normalized per metric ton of molten glass, analogous to Rahmat *et al.* (2025) [34]. The calculation includes the annualized CAPEX, derived from FCI, interest rate, and plant lifetime [79], in addition to operating expenditures (OPEX) and by-product sales. OPEX comprises both direct costs, such as process-required resources and energy, and indirect costs, including insurance, plant overhead, and contingencies. Labor costs are calculated based on the hourly wage (see Table 1) and an estimated annual labor input of 43,253 h, as described by Peters *et al.* (2003) [38]. Since CAPEX values only apply for the assumed plant size, NPC may vary from other estimations for different production capacities or plant locations. With CO_2 emissions contributing less than 4 t per year in the proposed plant design, we excluded CO_2 certificates from our calculations.

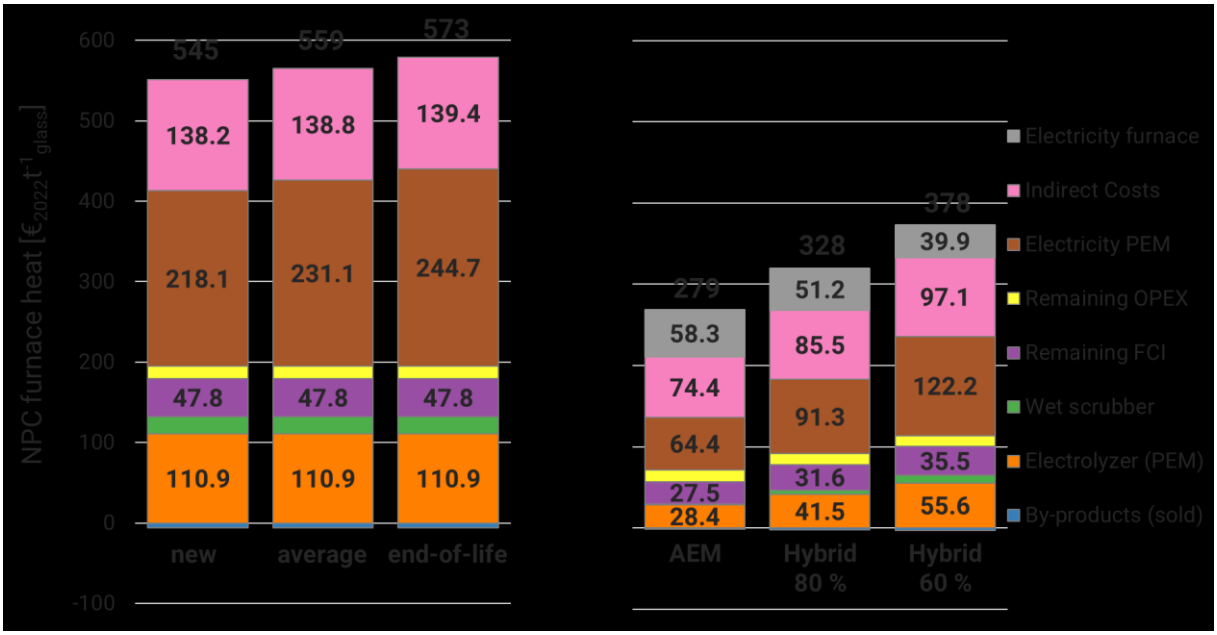

Figure 6. *(left) Net production costs (NPC) for furnace heat per MW SNG (LHV) of the process chain in a new, average-aged and end-of-life furnace. (right) NPC for furnace heat of other furnace technologies with a similar CCU process chain based on average-aged furnaces.*

At an average electricity price of €60 per MWh_{el} (2022), the average NPC per MW (LHV) furnace heat amounts to €559 per metric ton of molten glass (see Figure 6, left), compared to €128 per metric ton of molten glass for NG (€132 per MWh in 2022) [87]. Since the new glass furnace requires less energy, the NPC of SNG in the first year of operation amounts to €545 per metric ton of molten glass. Furnace degradation causes an increase in wall heat losses

over time, resulting in higher energy demand and consequently higher a NPC of SNG (€573 per metric ton molten glass).

In this scenario, electricity costs constitute approximately 41 % of the NPC, while the remaining direct OPEX contributes 3 %. The second-largest share is attributed to the PEM electrolyzer FCI, representing 20 % of the NPC. Other equipment FCI contributes 12 %, while indirect OPEX accounts for about 25 % of the total NPC. Electricity generated via SC is directly used to reduce the plant's total electricity demand. This results in an economic benefit as long as the average electricity price exceeds 54 € per MWh_{el}. Heat integration for district heating (DH) reduces overall NPC by 1 %. If the surplus SNG (3.7 kt / 53.9 GWh_{HHV} SNG per year) were sold at a market price of €125.72 per MWh_{HHV}, potential annual revenues of approximately €6.8M (2022) could be realized. In this case, the NPC would decrease to €497 per metric ton of molten glass, reflecting a 11 % reduction due to SNG sales.

Increasing the electrical energy input to the furnace leads to a significant decrease in the NPC of the furnace heat supply (see Figure 6, right). Simultaneously, the amount of recycled CO_2 decreases as the applied electricity increases, with no CO_2 recycling occurring in all-electric melter (AEM) furnaces. Given the furnace's requirement for electrical energy input, we added specific electricity costs ranging from €40 to €60 per metric ton molten of glass for improved comparison.

5.3 Process cycle with flexible hydrogen production

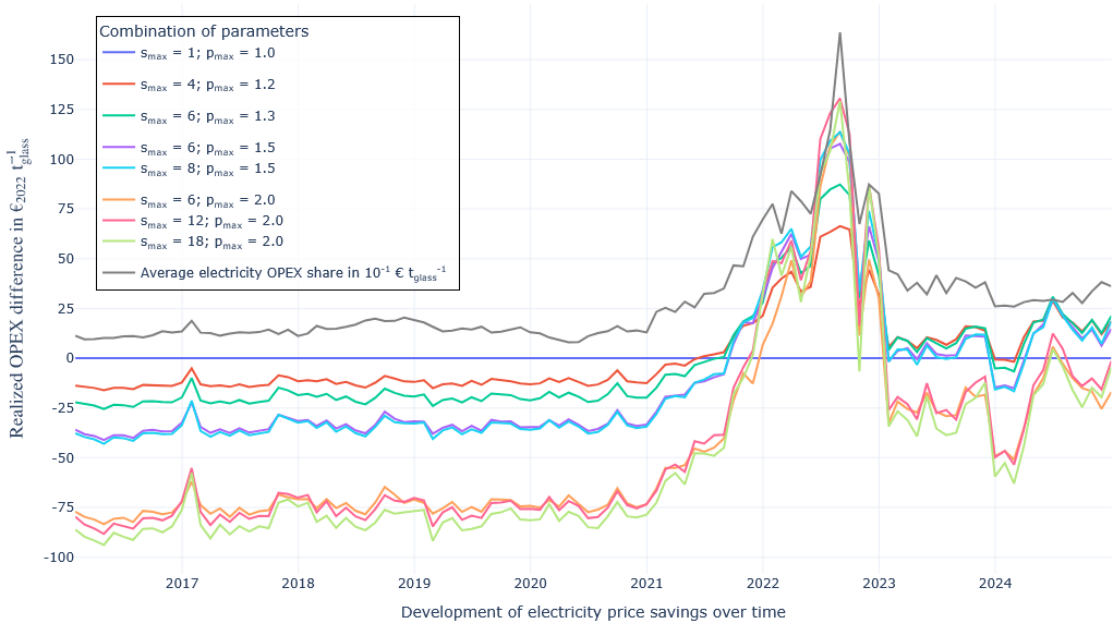

Figure 7. *Potential of OPEX reduction in respect of the standard case (s_{max} = 1 ; p_{max} = 1), with s_{max} as storage maximum and p_{max} as production maximum. For an interactive graph with further information, please look at the supplementary information.*

The algorithm described in section 2.3 enables a reduction in effective average electricity costs compared to spot market prices. This results in lower OPEX at the expense of higher FCI. In this example, we annualized the additional required equipment and added it to the electricity share of the NPC to illustrate the benefit of the process. Figure 7 shows potential OPEX savings in recent years when both electrolysis capacity (p_{max}, that is the electrolyzer capacity factor with 1 as standard case) and storage (s_{max}, that is storage capacity in hours) are increased. All

values above 0 (blue line) represent total NPC benefits, while values below represent disadvantageous production conditions. As the figure demonstrates, increasing electrolyzer capacity would not have provided economic benefits before 2021. However, with the sharp rise in electricity prices in 2022, larger electrolysis capacity improves economic feasibility compared to the standard configuration. In the standard case, there is enough storage for one hour of methanation and electrolyzer capacity to match methanation demand. At the same time, overall electricity costs have risen, which reduces general economic feasibility.

When plotting the effective electricity cost benefit against the average market price (Figure 8), a trend emerges. Increased financial benefit due to increased storage and electrolyzer capacities occurs during periods of high electricity market prices, leading to positive values for ΔElectricity costs (y). The intersection with the x-axis indicates the economic viability of storage and electrolyzer sizing. Smaller electrolyzer and storage capacities (for example 120 % electrolyzer capacity and 3 t hydrogen storage (sufficient for four hours of methanation, red line) are advantageous at electricity prices above €70 per MWh. Larger setups yield greater benefits at even higher prices. However, dynamic operation with increased capacities does not provide advantages below €70 per MWh.

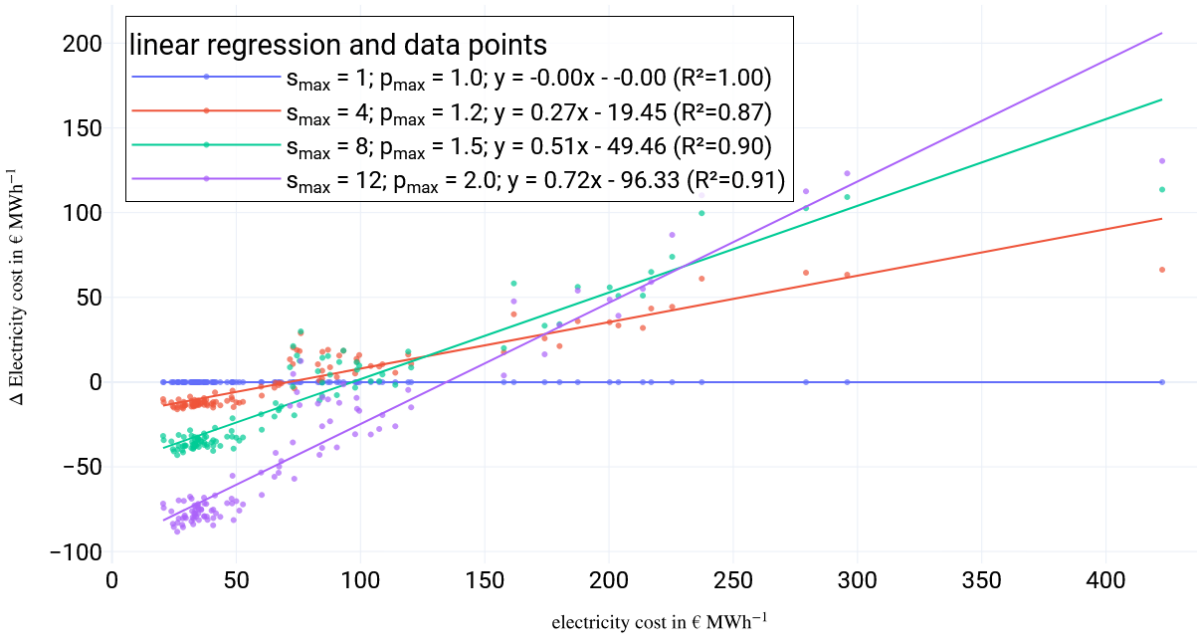

Figure 8. *Effective electricity prices in dependency of the market price.*

5.4 Sensitivity analysis at static electricity price conditions

The sensitivity analysis (**Figure 9**) illustrates the influence of electricity price on NPC_{SNG} (blue) and CO_2 abatement cost (red). The error bar of ± 30 % reflects the potential NPC_{SNG} range due to methodological uncertainty (representing plant size, efficiency assumptions and similar factors). We assumed scope 1 emissions of approximately 339 kg_{CO_2} per metric ton molten glass for natural gas combustion, including flue gas cooling and a wet scrubbing for comparability. With an average 2022 market price of €126 per MWh_{HHV} in addition to EU-ETS fees, natural gas (NG) combustion would thus lead to costs of €174 per metric ton molten glass.

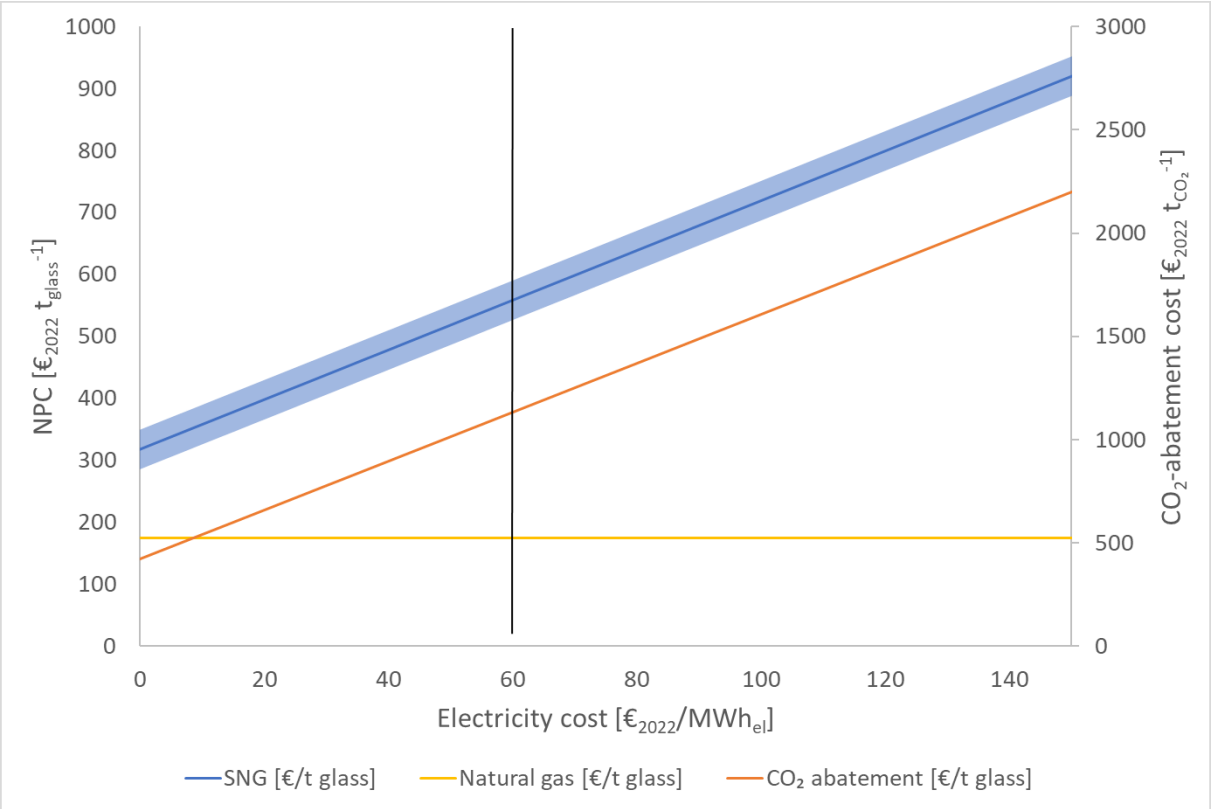

Figure 9. *Sensitivity analysis of NPC_{SNG} and CO_2-abatement cost with various electricity cost. Natural gas costs per metric ton molten gas (2022) were added for comparison.*

To compare CO_2 avoidance costs with contemporary processes, we relate costs of NG combustion to those of a CCU process at varying electricity prices. A competitive SNG based process chain without EU-ETS would require negative electricity prices of €-36 per MWh_{el}. At a typical electricity cost of €60 per MWh_{el}, the NPC_{SNG} is approximately 2.5 to 3.9 times higher than the average NG price**.** This results in CO_2 abatement costs of approximately €1,132 per metric ton of CO_2, based on scope 1 emissions from the process chain. Therefore, a significant increase in EU ETS prices is required to make the process chain economically viable. These abatement costs decrease slightly over time due to improved equipment utilization, ranging from €1,154 (new furnace) to €1,074 (end-of-life) per metric ton of CO_2. Considering that 2022 experienced particularly high energy prices in Germany, especially for NG, these abatement costs increase with lower NG prices and may reach up to €1,440 per metric ton of CO_2 at a gas price of €50 per MWh_{LHV}. Compared to other furnace technologies, CO_2 abatement costs remain similar for CO_2 abated through the CCU concept. However, the majority of CO_2 abatement (and thus the respective abatement costs) results from the furnace technology itself, reducing specific CO_2 emissions by 50 to 75 % compared to NG combustion. Since furnace parameters (costs, lifetime) were not included in this model, we cannot calculate abatement costs attributed to the furnace technology. In any case, we expect these abatement costs to be significantly lower than those calculated in our model.

6. Discussion

6.1 Economic and technological feasibility

Our study demonstrates that the technology required for carbon-neutral glass manufacturing is already available. Certain elements of the process chain, such as methanation, can even be outsourced to external suppliers or partners, which may reduce the complexity of flue gas treatment. Nevertheless, the techno-economic investigation indicates significantly higher costs compared to natural gas combustion in current glass production.

Given the substantial energy requirements under the assumed parameters, improving energy efficiency is a critical factor for the feasibility of the proposed process chain. Although scaling effects in methanation may enhance the economic viability of surplus conversion, they do not fully compensate for the inherent energy losses in fuel synthesis. Thus, measures that reduce chemical energy consumption in the furnace directly improve efficiency by a factor related to the power-to-heat efficiency. In our example, every MW reduction in fuel-based furnace energy consumption results in approximately 3 MW less required electrolysis capacity. Further improvements can be achieved by utilizing hydrogen directly for heating or by increasing the application of electric heating. Technological advances, such as hybrid furnaces that use up to 80 % electric energy input via electrodes (with energy efficiencies ranging from 80 to 95 % compared to approximately 40 to 65% for oxy-fuel combustion) will therefore increase overall energy efficiency. In contrast, traditional combustion-based heating, typically achieving efficiencies of about 30 to 55%, increases operational costs. This effect is reflected in the NPC shown in Figure 6, where increased electric input significantly decreases the NPC. Thus, from this perspective, the optimal path would be the application of AEM for container glass production. In an AEM process scenario, only a quarter of the total hydrogen (approximately 13 MW electrolysis capacity) would be required for the CCU process, while an additional 10 to 14 MW would be needed as electric energy input.

However, this simulation does not cover furnace parameters like NPC / CAPEX of the furnace technology and deviates further from the average lifetime of the respective furnace technology (AEM: about 7 years; hybrid furnaces: about 10 years [88]). AEM is further well established for certain glass types and smaller-scale operations, but its applicability remains limited for amber glass and large-scale production lines. Ongoing technological developments may expand its suitability in the future; for now, conventional or hybrid furnaces remain the most practical solutions for high-volume container and flat glass manufacturing. Importantly, these hybrid furnaces are compatible with the CCU process due to their similar design. In this context, less SNG would be required for heating, although surplus SNG formation would remain unchanged. Moreover, glass production with higher purity requirements and consequently lower cullet allowance can benefit from scaling effects, as these conditions are associated with higher CO_2 emissions.

6.2 Limitations due to space availability and furnace degradation

As the furnace degrades during operation, the demand for SNG and the CO_2 output in the furnace module increase. Therefore, increased production and processing capacities in the subsequent process chain must be considered, resulting in a higher CAPEX contribution to the NPC. In this model, we scaled the setup based on end-of-life furnace parameters, leaving hydrogen production capacities available during the early production years. Since PEM electrolyzers significantly affect overall NPC, optimization opportunities, such as temporarily selling production capacities, arise to reduce SNG production costs.

Furthermore, the modeled setup is constrained by spice requirements. Since calculating the exact area requirement falls outside the scope of this investigation, we present only rough estimations. The largest equipment by far is the PEM electrolyzer, occupying approximately 6,500 m² for a 50 MW unit [89]. We estimate the area for methanation reactors, the second largest equipment, to be between 500 and 1,000 m² [90]. Additional equipment, including wet scrubbers, NRU, hydrogenation units, and guard beds, occupies approximately 200 m².

6.3 Industrial synergies and sector coupling

The industrial transition towards a green economy is primarily driven by energy constraints. The efficiency of the electrolyzer unit is a key factor for the availability of hydrogen, both for the glass industry and for society as a whole. Electrolyzers with higher efficiency or the ability to use industrial waste heat are essential for a carbon-neutral process cycle. Recent progress with PEM electrolyzers are promising [91], and high-temperature electrolysis cells (SOEC) also

offer significant potential, as they can utilize the high waste heat from flue gas and methanation [92]. However, since our model is based on the technological status of 2022, alkaline electrolysis remains superior in terms of both CAPEX and efficiency.

Scaling effects can further reduce the costs of the proposed production cycle. For example, a daily production of 300 metric tons molten glass per day is typical for a container glass plants, and the methanation process was scaled accordingly. Float glass plants, in contrast, often reach up to 1,000 t molten glass per day, and require higher exergy input because of process-related higher dwelling times of the glass in the furnace. The float process also needs small amounts of hydrogen in the primary glass forming step, which could create synergies to hydrogen production. Scaling up of the methanation process, for example by combining the CO_2 output of different close-by industries, would lower its CAPEX share in the NPC_{SNG} and thus reduce the impact of the respective energy costs. Analogously, joint flue gas treatment with other industries, such as cement production, could further improve the efficiency of flue gas management.

6.4 Climate impact

Our proposed process chain significantly reduces global warming potential. For scope 1 and 2 emissions, values of 130 kg CO_2 per metric ton molten glass are achieved. The use of SNG lowers GWP by about 38 % compared to scope 1 and 2 emissions from natural gas combustion, which are around 339 kg CO_2 per metric ton molten glass in a comparable scenario. This benefit becomes even greater when scope 3.1 emissions from natural gas – arising from transport and extraction – are included, despite the higher overall energy demand of the process.

7. Summary

The suggested process cycle enables the abatement of more than 99 % of the scope 1 emissions at a glass production plant. When including scope 2 emissions associated with the electrolysis unit, the overall abatement is about 60 %, based on the prognosed energy mix of 2035 [27]. Although the interaction of all implemented technologies has not yet been fully investigated, each process step is well established in different industrial applications. Therefore, their integration should not pose major challenges for the process chain. However, the proposed process comes with several drawbacks, particularly regarding energy efficiency, use of rare elements, and, most importantly, economic viability. The combination of multiple technologies, such as wet lime scrubbing, nitrogen removal unit, hydrogenation, guard beds, methanation, and PEM electrolysis, result in a relatively high level of complexity. This complexity can be reduced by outsourcing certain steps to external partners. As the suggested process chain has not been thoroughly tested, we assessed a technological readiness level of 3, even though all selected technologies are industrially proven.

At the same time, the cost of energy supply for glass production at an average electricity price of €60 per MWh (2022) amounts to €559 per metric ton molten glass (2022). This is significantly more than the current cost of fossil energy, which was around €174 per metric ton molten glass in 2022. From a CO_2 abatement perspective, the proposed process chain leads to an increase in cost of €1,130 (2022) per metric ton CO_2 avoided. These costs are highly sensitive to the average electricity price. Although the capital cost share of expensive technologies like PEM electrolyzers may decrease with further development and scaling, the overall impact on NPC_{SNG} remains limited due to the high OPEX share.

The economic feasibility of dynamic hydrogen production with additional storage solutions also depends on the average electricity price. While the OPEX share may decrease, the increased annualized capital costs can raise the NPC_{SNG} due to high investment requirements. Historical electricity market data show that this approach only becomes financially beneficial if

the average electricity price exceeds €70 per MWh. Since this mode of operation benefits from a highly volatile electricity market, its prospects may improve as the share of renewable electricity increases.

We have demonstrated that CO_2-neutral (scope 1) glass production is technically feasible using available technologies, despite the high NPC_{SNG} for the modeled system compared to current glass production. The GWP benefit persists even when additional scope 2 emissions of approximately 130 t CO_2 per metric ton molten glass are considered. The study provides a baseline for decision-making regarding options to defossilize glass production and highlights the challenges that lie ahead. While we do not consider the proposed model to be a viable industry standard at present, it establishes a foundation for future developments.

Looking ahead, the glass industry faces a decisive transformation as it strives for climate neutrality by 2045. While electrification and hydrogen-based melting are advancing rapidly, addressing residual process-related CO_2 emissions remains a key challenge. Our study demonstrates that CCU-based closed carbon cycles can complement existing approaches by targeting these unavoidable emissions, particularly in segments with limited cullet availability or high-quality requirements. Realizing such solutions will require further progress in CO_2 capture technology, infrastructure, and access to affordable renewable energy. By evaluating technical feasibility and identifying the main barriers to closed carbon cycles, this study supports the glass industry's path toward full defossilization. As the industry innovates to meet regulatory pressure, customer expectations, and maintain long-term competitiveness, collaboration across the value chain and targeted policy support will be essential. This will ensure that all defossilization options, including closed carbon cycles, can be effectively implemented at scale.

Disclaimer

The authors used Perplexity AI, which leverages OpenAI's GPT-4 language model, to assist with literature research and editorial suggestions. Additionally, AI tools supported the development of the underlying Python models for scientific calculations. All sources identified through AI-assisted literature research were independently verified by the authors. The authors are solely responsible for the scientific accuracy, originality, and interpretation of the results. AI support complements but does not replace the author's expertise, critical judgment, or accountability. Never underestimate the ability of the AI to feed you incorrect information!

The authors declare that they have no competing interests.

Acknowledgements

The authors would like to express the gratitude to the German Federal Ministry of Education and Research for the granted funding in the "KlimPro-Industrie"-call (Grant no. 01LJ2005 A and B) and the NextGenerationEU program to conduct the GlasCO2 project. Our gratitude is also addressed to the associated partners in the GlasCO2 project, particularly Ardagh Glass GmbH, Schott AG and Linde AG. The authors would also like to thank Clariant AG for the discussions held during the GlasCO2 project.

References

[1] L. Kemp *et al.*, 'Climate Endgame: Exploring catastrophic climate change scenarios', *Proc. Natl. Acad. Sci. U.S.A.*, vol. 119, no. 34, p. e2108146119, Aug. 2022, doi: 10.1073/pnas.2108146119.

[2] M. Kotz, A. Levermann, and L. Wenz, 'The economic commitment of climate change', *Nature*, vol. 628, no. 8008, pp. 551–557, Apr. 2024, doi: 10.1038/s41586-024-07219-0.

[3] United Nations, *The Paris Agreement*, vol. FCCC/CP/2015/L.9/Rev.1. 2016. [Online]. Available: https://unfccc.int/sites/default/files/resource/parisagreement_publication.pdf
[4] N. J. L. Lenssen *et al.*, 'Improvements in the GISTEMP Uncertainty Model', *JGR Atmospheres*, vol. 124, no. 12, pp. 6307–6326, Jun. 2019, doi: 10.1029/2018JD029522.
[5] A. D. Ellerman and B. K. Buchner, 'The European Union Emissions Trading Scheme: Origins, Allocation, and Early Results', *Review of Environmental Economics and Policy*, vol. 1, no. 1, pp. 66–87, Jan. 2007, doi: 10.1093/reep/rem003.
[6] P. Bayer and M. Aklin, 'The European Union Emissions Trading System reduced CO_2 emissions despite low prices', *Proc. Natl. Acad. Sci. U.S.A.*, vol. 117, no. 16, pp. 8804–8812, Apr. 2020, doi: 10.1073/pnas.1918128117.
[7] 'Inventory of U.S. Greenhouse Gas Emissions and Sinks: 1990-2022', U. S. Environmental Protection Agency, EPA, EPA 430R-24004, 2024.
[8] G. Ganti *et al.*, 'Evaluating the near- and long-term role of carbon dioxide removal in meeting global climate objectives', *Commun Earth Environ*, vol. 5, no. 1, p. 377, Jul. 2024, doi: 10.1038/s43247-024-01527-z.
[9] P. Javadi *et al.*, 'The impact of regional resources and technology availability on carbon dioxide removal potential in the United States', *Environ. Res.: Energy*, vol. 1, no. 4, p. 045007, Dec. 2024, doi: 10.1088/2753-3751/ad81fb.
[10] M. Abegg, Z. Clulow, L. Nava, and D. M. Reiner, 'Expert insights into future trajectories: assessing cost reductions and scalability of carbon dioxide removal technologies', *Front. Clim.*, vol. 6, p. 1331901, May 2024, doi: 10.3389/fclim.2024.1331901.
[11] Y. Erbay and A. Mattos, 'Global Assessment of Direct Air Capture Costs', IEAGHG, Cheltenham, Dec. 2021.
[12] K. Sievert, T. S. Schmidt, and B. Steffen, 'Considering technology characteristics to project future costs of direct air capture', *Joule*, vol. 8, no. 4, pp. 979–999, Apr. 2024, doi: 10.1016/j.joule.2024.02.005.
[13] J. Young *et al.*, 'The cost of direct air capture and storage can be reduced via strategic deployment but is unlikely to fall below stated cost targets', *One Earth*, vol. 6, no. 7, pp. 899–917, Jul. 2023, doi: 10.1016/j.oneear.2023.06.004.
[14] M. Crippa *et al.*, 'GHG emissions of all world countries.', Luxembourg, JRC138862, 2024. Accessed: Jan. 10, 2025. [Online]. Available: https://data.europa.eu/doi/10.2760/4002897
[15] J. Egerer, N. Farhang-Damghani, V. Grimm, and P. Runge, 'The industry transformation from fossil fuels to hydrogen will reorganize value chains: Big picture and case studies for Germany', *Applied Energy*, vol. 358, p. 122485, Mar. 2024, doi: 10.1016/j.apenergy.2023.122485.
[16] L. Holappa, 'A General Vision for Reduction of Energy Consumption and CO_2 Emissions from the Steel Industry', *Metals*, vol. 10, no. 9, p. 1117, Aug. 2020, doi: 10.3390/met10091117.
[17] E. Benhelal, E. Shamsaei, and M. I. Rashid, 'Challenges against CO_2 abatement strategies in cement industry: A review', *Journal of Environmental Sciences*, vol. 104, pp. 84–101, Jun. 2021, doi: 10.1016/j.jes.2020.11.020.
[18] D. D. Furszyfer Del Rio *et al.*, 'Decarbonizing the glass industry: A critical and systematic review of developments, sociotechnical systems and policy options', *Renewable and Sustainable Energy Reviews*, vol. 155, p. 111885, Mar. 2022, doi: 10.1016/j.rser.2021.111885.
[19] European Environment Agency, 'EU Emissions Trading System (ETS) data viewer', European Environment Agency. Accessed: Jan. 10, 2025. [Online]. Available: https://www.eea.europa.eu/en/analysis/maps-and-charts/emissions-trading-viewer-1-dashboards
[20] W. Dienemann, 'HEIDELBERG MATERIALS' CO_2 roadmap On the way to carbon neutrality', *ce papers*, vol. 6, no. 6, pp. 110–113, Dec. 2023, doi: 10.1002/cepa.2819.
[21] T. A. Branca, V. Colla, M. M. Murri, and A. J. Schröder, 'The Impact of the New Technologies and the EU Climate Objectives on the Steel Industry', in *Industry 4.0 and the Road to Sustainable Steelmaking in Europe*, D. Stroud, A. J. Schröder, L. Antonazzo, C. Behrend, V. Colla, A. Goti, and M. Weinel, Eds., in Topics in Mining, Metallurgy and Materials

Engineering. , Cham: Springer International Publishing, 2024, pp. 53–75. doi: 10.1007/978-3-031-35479-3_4.
[22] Nippon Sheet Glass Co., Ltd., 'Architectural glass production powered by hydrogen in world first', pilkington.com. Accessed: Jan. 10, 2025. [Online]. Available: https://www.pilkington.com/en-gb/uk/news-insights/latest/architectural-glass-production-powered-by-hydrogen-in-world-first
[23] Lars Biennek, 'All-electric melting prospects for glass container production', *Glass Worldwide*, vol. 88, pp. 76–80, 2020.
[24] Ardagh Glass Packaging, 'Ardagh Glass Packaging welcomes glass industry partners to NextGen Furnace launch', *Glass Technology: European Journal of Glass Science and Technology Part A*, vol. 64, no. 6, pp. 202–203, 2023.
[25] C. Sinton, 'Deep decarbonization of glassmaking', *American Ceramic Society Bulletin*, vol. 102, p. 24, May 2023.
[26] FEVE, 'Recycling: why glass always has a happy CO_2 ending', FEVE, Brussels, 2016. [Online]. Available: https://feve.org/wp-content/uploads/2016/04/FEVE-brochure-Recycling-Why-glass-always-has-a-happy-CO2-ending-.pdf
[27] British Glass, 'Glass sector. Net zero strategy 2050', 2019.
[28] P. Leisin and P. Radgen, 'Glas 2045 - Dekarbonatisierung der Glasindustrie', IER Institut für Energiewirtschaft und Rationelle Energieanwendung, Stuttgart, Studie im Auftrag des Bundesverband Glasindustrie e.V., 2022.
[29] M. Zier, P. Stenzel, L. Kotzur, and D. Stolten, 'A review of decarbonization options for the glass industry', *Energy Conversion and Management: X*, vol. 10, p. 100083, Jun. 2021, doi: 10.1016/j.ecmx.2021.100083.
[30] FEVE, 'Latest glass packaging recycling rate steady at 76%'. Accessed: Jul. 14, 2025. [Online]. Available: https://feve.org/glass_recycling_stats_2018/
[31] O-I ITALY SPA, Stazione sperimentale del vetro societa consortile per azioni, and K2-CO2 SRL, 'Full-scale demonstration of carbon capture and storage in glass manufacturing to limit furnace CO2 emissions', Varese, Project description LIFE23-CCM-IT-GLASS2LIFE/101158029, 06/2028 2025. [Online]. Available: https://webgate.ec.europa.eu/life/publicWebsite/project/LIFE23-CCM-IT-GLASS2LIFE-101158029/full-scale-demonstration-of-carbon-capture-and-storage-in-glass-manufacturing-to-limit-furnace-co2-emissions#
[32] R. Ireson *et al.*, 'Renewable waste-derived fuels for glass and ceramics manufacturing: feasibility study', A report for Department for Business, Energy & Industrial Strategy, 2023. [Online]. Available: https://assets.publishing.service.gov.uk/media/649ac491b4d6ef000c038f5e/Glass_Futures_-_IFS_Phase_1_report.pdf
[33] Bundesverband Erneuerbare Energie e.V., 'Erneuerbare Energien als Schlüssel für Deutschlands Wohlstand', BEE, Berlin, Positionspapier, Dec. 2024. [Online]. Available: https://www.bee-ev.de/service/publikationen-medien/beitrag/erneuerbare-energien-als-schluessel-fuer-deutschlands-wohlstand
[34] Y. Rahmat, F. Drünert, B. Fleischmann, and R.-U. Dietrich, 'Advancing the defossilization of the glass industry based on the integration of synthetic fuels production', *Fuel*.
[35] Bundesministerium für Wirtschaft und Klimaschutz, 'Wettbewerbsfähige Strompreise für die energieintensiven Unternehmen in Deutschland und Europa sicherstellen', BMWK, Berlin, Arbeitspapier des BMWK zum Industriestrompreis für das Treffen Bündnis Zukunft der Industrie, May 2023.
[36] E. Althoff *et al.*, 'Climate-neutral power system 2035. How the German power sector can become climate-neutral by 2035', Agora Energiewende, Prognos, Consentec, Berlin, 267/02-ES-2022/EN, 2022. [Online]. Available: https://www.agora-energiewende.org/publications/climate-neutral-power-system-2035-summary
[37] T. Lauf, M. Memmler, and S. Schneider, 'Emissionsbilanz erneuerbarer Energieträger 2023', Umweltbundesamt, Dessau-Roßlau, Mar. 2025. doi: 10.60810/OPENUMWELT-7687.
[38] M. S. Peters, K. D. Timmerhaus, R. E. West, and R. E. West, *Plant design and economics for chemical engineers*, 5. ed., International ed. in McGraw-Hill chemical engineering series. Boston: McGraw-Hill, 2003.

[39] BDEW, 'BDEW-Gaspreisanalyse April 2023', Berlin, Apr. 2023. [Online]. Available: https://www.bdew.de/media/original_images/2023/04/25/230420_bdew-gaspreisanalyse_april-2023_20042023.pdf
[40] C. Jatzwauk, 'Design and Operation of Glass Furnaces', in *Encyclopedia of Glass Science, Technology, History, and Culture*, 1st ed., P. Richet, R. Conradt, A. Takada, and J. Dyon, Eds., Wiley, 2021, pp. 1147–1164. doi: 10.1002/9781118801017.ch9.7.
[41] B. M. Scalet, M. Garcia Muñoz, A. Q. Sissa, S. Roudier, and L. Delgado Sancho, 'Best available techniques (BAT) reference document for the manufacture of glass: industrial emissions Directive 2010/75/EU: integrated pollution prevention and control.', Joint Research Centre of the European Commission, Luxembourg, 2013. Accessed: Jan. 10, 2025. [Online]. Available: https://data.europa.eu/doi/10.2791/69502
[42] Madivate, Carvalho, Müller, Franz, and Wilsmann, Wolfgang, 'Thermochemistry of the glass melting process - Energy requirement in melting soda-lime-silica glasses from cullet-containing batches', *Glastech. Ber. Glass Sci. Technol.*, vol. 69, no. 6, pp. 167–178, 1996.
[43] Reinhard Conradt, *Thermodynamik und Glas*, 2nd ed. in Handbuch der Glastechnik. Offenbach am Main: Verlag der Deutschen Glastechnischen Gesellschaft e. V., 2022.
[44] S. Rezaei, A. Liu, and P. Hovington, 'Emerging technologies in post-combustion carbon dioxide capture & removal', *Catalysis Today*, vol. 423, p. 114286, Nov. 2023, doi: 10.1016/j.cattod.2023.114286.
[45] E. Mostafavi, O. Ashrafi, and P. Navarri, 'Assessment of process modifications for amine-based post-combustion carbon capture processes', *Cleaner Engineering and Technology*, vol. 4, p. 100249, Oct. 2021, doi: 10.1016/j.clet.2021.100249.
[46] J. Tian, Y. Shen, D. Zhang, and Z. Tang, 'CO_2 capture by vacuum pressure swing adsorption from dry flue gas with a structured composite adsorption medium', *Journal of Environmental Chemical Engineering*, vol. 9, no. 5, p. 106037, Oct. 2021, doi: 10.1016/j.jece.2021.106037.
[47] M. T. Ho, G. W. Allinson, and D. E. Wiley, 'Reducing the Cost of CO_2 Capture from Flue Gases Using Pressure Swing Adsorption', *Ind. Eng. Chem. Res.*, vol. 47, no. 14, pp. 4883–4890, Jul. 2008, doi: 10.1021/ie070831e.
[48] J. Gao, S. Wang, J. Wang, L. Cao, S. Tang, and Y. Xia, 'Effect of SO_2 on the amine-based CO_2 capture solvent and improvement using ion exchange resins', *International Journal of Greenhouse Gas Control*, vol. 37, pp. 38–45, Jun. 2015, doi: 10.1016/j.ijggc.2015.03.001.
[49] S. Talei, D. Fozer, P. S. Varbanov, A. Szanyi, and P. Mizsey, 'Oxyfuel Combustion Makes Carbon Capture More Efficient', *ACS Omega*, p. acsomega.3c05034, Jan. 2024, doi: 10.1021/acsomega.3c05034.
[50] J. L. Sorrels, A. Baynham, D. D. Randall, and R. Laxton, 'Section 5: Wet and dry scrubbers for acid gas control', in *Cost reports and guidance for air pollution regulations*, 7th ed., United States Environmental Protection Agency, Ed., Research Triangle Park, NC.
[51] K. Daginnus, T. Marty, N. V. Trotta, T. Brinkmann, A. Whitfield, and S. Roudier, 'Best available techniques (BAT) reference document for common waste gas management and treatment systems in the chemical sector: Industrial Emissions Directive 2010/75/EU (integrated pollution prevention and control)', Joint Research Centre of the European Commission, Luxembourg, JRC131915, Jan. 2023. Accessed: Jan. 10, 2025. [Online]. Available: https://data.europa.eu/doi/10.2760/220326
[52] Aurora Energy, LLC, 'Best Available Control Technology Analysis, Chena Power Plant, Fairbanks, Alaska', Cincinnati, OH, 2019. [Online]. Available: https://dec.alaska.gov/media/5y1jydex/chena-bact-determination.pdf
[53] M. Z. Zuwairi and S. A. Rahman, 'Study on CO_2 / N_2 separation: the effect of rubbery polymer coating on PVDF membrane', *IOP Conf. Ser.: Mater. Sci. Eng.*, vol. 206, p. 012047, Jun. 2017, doi: 10.1088/1757-899X/206/1/012047.
[54] I. A. Hashim *et al.*, 'Separation of CO_2 from nitrogen and oxygen using hydrophobic ceramic membrane', *Journal of Applied Material Science & Engineering Research*, vol. 7, no. 2, pp. 172–181, Oct. 2023, doi: 10.20944/preprints202310.1113.v1.

[55] J. C. Kuo, K. H. Wang, and C. Chen, 'Pros and cons of different Nitrogen Removal Unit (NRU) technology', *Journal of Natural Gas Science and Engineering*, vol. 7, pp. 52–59, Jul. 2012, doi: 10.1016/j.jngse.2012.02.004.
[56] M. Samei and A. Raisi, 'Separation of nitrogen from methane by multi-stage membrane processes: Modeling, simulation, and cost estimation', *Journal of Natural Gas Science and Engineering*, vol. 98, p. 104380, Feb. 2022, doi: 10.1016/j.jngse.2021.104380.
[57] M. C. Flores and K. C. D. S. Figueiredo, 'Carbon Dioxide/Nitrogen Separation Through Oxygenated Carbon Nanotubes-Containing Polysulfone Membranes', *Macromolecular Symposia*, vol. 394, no. 1, p. 2000058, Dec. 2020, doi: 10.1002/masy.202000058.
[58] R. Doctor *et al.*, 'Transport of CO_2', in *IPCC Special Report on Carbon Dioxide Capture and Storage*, Intergovernmental Panel on Climate Change (IPCC), Ed., Cambridge: Cambridge University Press, 2005, pp. 179–194. [Online]. Available: https://www.ipcc.ch/site/assets/uploads/2018/03/srccs_chapter4-1.pdf
[59] J. Race, B. Wetenhall, P. N. Seevam, and M. J. Downie, 'Towards a CO_2 pipeline specification: defining tolerance', *The Journal of Pipeline Engineering*, vol. 11, no. 3, pp. 173–190, 2012.
[60] T. Roeder, A. Rosenstiel, N. Monnerie, and C. Sattler, 'Impact of expected cost reduction and lifetime extension of electrolysis stacks on hydrogen production costs', *International Journal of Hydrogen Energy*, vol. 95, pp. 1242–1251, Dec. 2024, doi: 10.1016/j.ijhydene.2024.08.015.
[61] T. D. Fechtenburg, 'The Value of Flexibility for Electrolyzers', energinet, Fredericia, 22/04134–1, May 2022. Accessed: Jan. 17, 2025. [Online]. Available: https://energinet.dk/media/essfy3sk/the-value-of-flexibility-for-electrolyzers-thomas-dalgas-fechtenburg-energinet.pdf
[62] C. Moran *et al.*, 'A flexible techno-economic analysis tool for regional hydrogen hubs – A case study for Ireland', *International Journal of Hydrogen Energy*, vol. 48, no. 74, pp. 28649–28667, Aug. 2023, doi: 10.1016/j.ijhydene.2023.04.100.
[63] O. Schmidt, A. Gambhir, I. Staffell, A. Hawkes, J. Nelson, and S. Few, 'Future cost and performance of water electrolysis: An expert elicitation study', *International Journal of Hydrogen Energy*, vol. 42, no. 52, pp. 30470–30492, Dec. 2017, doi: 10.1016/j.ijhydene.2017.10.045.
[64] M. Kopp, D. Coleman, C. Stiller, K. Scheffer, J. Aichinger, and B. Scheppat, 'Energiepark Mainz: Technical and economic analysis of the worldwide largest Power-to-Gas plant with PEM electrolysis', *International Journal of Hydrogen Energy*, vol. 42, no. 19, pp. 13311–13320, May 2017, doi: 10.1016/j.ijhydene.2016.12.145.
[65] M. Sánchez, E. Amores, D. Abad, L. Rodríguez, and C. Clemente-Jul, 'Aspen Plus model of an alkaline electrolysis system for hydrogen production', *International Journal of Hydrogen Energy*, vol. 45, no. 7, pp. 3916–3929, Feb. 2020, doi: 10.1016/j.ijhydene.2019.12.027.
[66] F. Habermeyer, V. Papantoni, U. Brand-Daniels, and R.-U. Dietrich, 'Sustainable aviation fuel from forestry residue and hydrogen – a techno-economic and environmental analysis for an immediate deployment of the PBtL process in Europe', *Sustainable Energy Fuels*, vol. 7, no. 17, pp. 4229–4246, 2023, doi: 10.1039/D3SE00358B.
[67] K. Stangeland, D. Kalai, H. Li, and Z. Yu, 'CO_2 Methanation: The Effect of Catalysts and Reaction Conditions', *Energy Procedia*, vol. 105, pp. 2022–2027, May 2017, doi: 10.1016/j.egypro.2017.03.577.
[68] H. Harms, B. Höhlein, and A. Skov, 'Methanisierung kohlenmonoxidreicher Gase beim Energie-Transport', *Chemie Ingenieur Technik*, vol. 52, no. 6, pp. 504–515, Jan. 1980, doi: 10.1002/cite.330520605.
[69] É. S. Van-Dal and C. Bouallou, 'Design and simulation of a methanol production plant from CO_2 hydrogenation', *Journal of Cleaner Production*, vol. 57, pp. 38–45, Oct. 2013, doi: 10.1016/j.jclepro.2013.06.008.
[70] C. H. Bartholomew, 'Mechanisms of Nickel Catalyst Poisoning', in *Studies in Surface Science and Catalysis*, vol. 34, Elsevier, 1987, pp. 81–104. doi: 10.1016/S0167-2991(09)60352-9.

[71] K.-T. Li and Y.-C. Hung, 'Hydrogenation of sulfur dioxide to hydrogen sulfide over Fe/γ-Al_2O_3 catalysts', *Applied Catalysis B: Environmental*, vol. 40, no. 1, pp. 13–20, Jan. 2003, doi: 10.1016/S0926-3373(02)00009-7.
[72] D. Chiche, C. Diverchy, A.-C. Lucquin, F. Porcheron, and F. Defoort, 'Synthesis Gas Purification', *Oil Gas Sci. Technol. – Rev. IFP Energies nouvelles*, vol. 68, no. 4, pp. 707–723, Jul. 2013, doi: 10.2516/ogst/2013175.
[73] A. Coy and T. Cotter, 'Personal Conversation about Requirements and Usage of Catalysts at Clariant', Sep. 09, 2021.
[74] S. Rönsch *et al.*, 'Review on methanation – From fundamentals to current projects', *Fuel*, vol. 166, pp. 276–296, Feb. 2016, doi: 10.1016/j.fuel.2015.10.111.
[75] R. Bellman, *Dynamic programming*. Princeton, NJ: Princeton Univ. Pr, 1957.
[76] D. P. Bertsekas, *Dynamic programming and optimal control*, 4th edition. in Athena scientific optimization and computation series. Nashua, NH: Athena scientific, 2012.
[77] A. S. Mehr, A. D. Phillips, M. P. Brandon, M. T. Pryce, and J. G. Carton, 'Recent challenges and development of technical and technoeconomic aspects for hydrogen storage, insights at different scales; A state of art review', *International Journal of Hydrogen Energy*, vol. 70, pp. 786–815, Jun. 2024, doi: 10.1016/j.ijhydene.2024.05.182.
[78] A. Alekseev *et al.*, 'Hydrogen liquefaction, storage, transport and application of liquid hydrogen', Karlsruher Institut für Technologie (KIT), 2023. doi: 10.5445/IR/1000168281.
[79] F. G. Albrecht, D. H. König, N. Baucks, and R.-U. Dietrich, 'A standardized methodology for the techno-economic evaluation of alternative fuels – A case study', *Fuel*, vol. 194, pp. 511–526, Apr. 2017, doi: 10.1016/j.fuel.2016.12.003.
[80] S. Maier, S. Tuomi, J. Kihlman, E. Kurkela, and R.-U. Dietrich, 'Techno-economically-driven identification of ideal plant configurations for a new biomass-to-liquid process – A case study for Central-Europe', *Energy Conversion and Management*, vol. 247, p. 114651, Nov. 2021, doi: 10.1016/j.enconman.2021.114651.
[81] Martin Kopp, 'Strommarktseitige Optimierung des Betriebs einer PEM-Elektrolyseanlage', Uni Kassel, Kassel, 2018.
[82] D. Ruprecht, 'Rohstoffbedarf der Wasserstoffproduktion', Ffe Beitragsreihe Wasserstoff Deep Dives. Accessed: May 15, 2025. [Online]. Available: https://www.ffe.de/veroeffentlichungen/beitragsreihe-wasserstoff-deep-dives-rohstoffbedarf-der-wasserstoffproduktion/
[83] F. D. Meylan, V. Moreau, and S. Erkman, 'Material constraints related to storage of future European renewable electricity surpluses with CO_2 methanation', *Energy Policy*, vol. 94, pp. 366–376, Jul. 2016, doi: 10.1016/j.enpol.2016.04.012.
[84] A. Schwochow, 'Betriebliche CO_2-Bilanz - Scopes leicht erklärt', KliMaWirtschaft. Accessed: Mar. 25, 2025. [Online]. Available: https://klimaschutz-wirtschaft.de/greenhouse-gas-protocol-scopes-leicht-erklaert/
[85] D. R. Woods, *Rules of Thumb in Engineering Practice*, 1st ed. Wiley, 2007. doi: 10.1002/9783527611119.
[86] G. Parks, R. Boyd, J. Cornish, and R. Remick, 'Hydrogen Station Compression, Storage, and Dispensing Technical Status and Costs Independent Review', National Renewable Energy Laboratory, Denver West Parkway, technical report NREL/BK-6A10-58564, 2014. Accessed: Jan. 10, 2025. [Online]. Available: http://rgdoi.net/10.13140/RG.2.2.23768.34562
[87] 'EU Natural Gas', Trading Economics. Accessed: May 09, 2025. [Online]. Available: https://tradingeconomics.com/commodity/eu-natural-gas
[88] Biennek, Lars *et al.*, 'HVG-Fortbildungskurs 2025: Ofenbau für die Glasherstellung', Hanau-Steinheim, Nov. 24, 2025.
[89] Coleman, David *et al.*, 'Wasserstoff-Potenzialstudie und -Bewertung einer versiegelten Industriefläche am Beispiel "Rüsselsheim West"', Wiesbaden, Final report, Sep. 2025. [Online]. Available: https://www.ruesselsheim.de/medien/pdfs-ruesselsheim.de/wirtschaft/2025-wasserstoff-potenzialstudie-ruesselsheim-west-hynes-cruh21.pdf
[90] Baum, Wolfgang, Bayer, Thomas, Horn, Elmar, Lienkamp, Heinrich, and Rastogi, Ashok, 'Auslegung, Bau und Betrieb von 5 MW und 20 MW Methanisierungsanlagen für das Energiespeicherkonzept "Power to Gas" - eine Vorstudie', Infraserv Höchst, Frankfurt am

Main, Abschlussbericht FKZ 0325627, Dec. 2014. [Online]. Available: https://edocs.tib.eu/files/e01fb15/842184619.pdf

[91] A. H. Reksten, M. S. Thomassen, S. Møller-Holst, and K. Sundseth, 'Projecting the future cost of PEM and alkaline water electrolysers; a CAPEX model including electrolyser plant size and technology development', *International Journal of Hydrogen Energy*, vol. 47, no. 90, pp. 38106–38113, Nov. 2022, doi: 10.1016/j.ijhydene.2022.08.306.

[92] Y. Li, L. Zhang, B. Yu, J. Zhu, and C. Wu, 'CO_2 High-Temperature Electrolysis Technology Toward Carbon Neutralization in the Chemical Industry', *Engineering*, vol. 21, pp. 101–114, Feb. 2023, doi: 10.1016/j.eng.2022.02.016.